FACULTY
OF MATHEMATICS
AND PHYSICS
Charles University

BACHELOR THESIS

Radek Folprecht

Many-body methods within the nuclear Lipkin model

Institute of Particle and Nuclear Physics

Supervisor of the bachelor thesis: Mgr. František Knapp Ph.D.

Study programme: Physics

Study branch: Physics

Prague 2023

I declare that I carried out this bachelor thesis independently, and only with the cited sources, literature and other professional sources. It has not been used to obtain another or the same degree.

I understand that my work relates to the rights and obligations under the Act No. 121/2000 Sb., the Copyright Act, as amended, in particular the fact that the Charles University has the right to conclude a license agreement on the use of this work as a school work pursuant to Section 60 subsection 1 of the Copyright Act.

In . . . . date . . . .

<div align="right">Author's signature</div>

iii

Title: Many-body methods within the nuclear Lipkin model

Author: Radek Folprecht

Institute: Institute of Particle and Nuclear Physics

Supervisor: Mgr. František Knapp Ph.D., Institute of Particle and Nuclear Physics

Abstract: The subject of the present thesis is the Lipkin model, a two-level degenerated quantum system enhanced by two-body interactions. The exact solutions and properties of the model are reviewed and summarized. Several many-body methods common in nuclear physics are used to solve the eigenvalue problem of the time-independent Schrödinger equation. The many-body methods applied to the Lipkin model in the present thesis are the Hartree-Fock mean-field method, the random phase approximation, the Tamm-Dancoff approximation, and the Bardeen-Cooper-Schrieffer method. We propose an instructive iterative extension to the random phase approximation method. For the listed methods, we provide a comprehensive comparison of the approximation quality for either the ground state energy or excited state energies.

Keywords: Lipkin model, Hartree-Fock mean-field method, random phase approximation, Bardeen-Cooper-Schrieffer method

Název práce: Mnohočásticové metody v jaderném Lipkinově modelu

Autor: Radek Folprecht

Ústav: Ústav částicové a jaderné fyziky

Vedoucí bakalářské práce: Mgr. František Knapp Ph.D., Ústav částicové a jaderné fyziky

Abstrakt: Předmětem předkládané práce je studium Lipkinova modelu - degenerovaného dvouhladinového systému zahrnujícího dvoučásticové interakce. Práce obsahuje stručné shrnutí a diskusi exaktních řešení tohoto modelu a jejich vlastností. Dále se zabýváme otázkou řešení stacionární Schrödingerovy rovnice odpovídající tomuto modelu pomocí běžně užívaných mnohočásticových metod jaderné fyziky. Tato práce se zabývá aplikací následujících metod: Hartree-Fockovou metodou středního pole, aproximací náhodnou fází, Tamm-Dancoffovou aproximací a Bardeen-Cooper-Schriefferovou metodou. Práce dále zahrnuje nové iterativní rozšíření aproximace náhodou fází, které je na tomto modelu vyzkoušeno. Výsledky všech těchto aproximací pro energie základního stavu případně stavů excitovaných jsou pak v rámci práce systematicky porovnány.

Klíčová slova: Lipkinův model, Hartree-Fockova metoda středního pole, aproximace náhodnou fází, Bardeen-Cooper-Schriefferova metoda

Contents

Introduction

The Lipkin model is a very appealing and, to this day, very popular model for quantum many-body systems. Thanks to its simplicity, exact solutions to the model exist first proposed in [1–3], or they can be easily found numerically. In contemporary physics, the model is commonly a subject of study in areas such as condensed matter physics [4], the quantum optics [5] or the quantum computing [6]. In this context, the model is often treated as an open quantum system [7].

However, the model was originally proposed in [1–3] so that various many-body methods could be tested in it, and the results directly compared with exact solutions. The Lipkin model lived up to its original intention, and dozens of many-body methods were applied and studied specifically on this model or some of its extensions. Examples of these methods are the Hartree-Fock method [8–10], the random phase approximation [11], the second random phase approximation [12] or various beyond mean-field methods [13–16].

In the present thesis, in Chapter 1, we first introduce the Lipkin model. Aside from exact solutions, we show some of the model's physical features. Among these are phase transitions and the odd-even effect analogy [8]. Next, we review some of the usual many-body methods used in nuclear physics, namely the Hartree-Fock method in Chapter 2 and the random phase approximation in Chapter 3, and we apply these methods to the Lipkin model. A detailed discussion regarding the properties of the Hartree-Fock and random phase approximation solutions is given. We establish and discuss a connection between the phase transitions and random phase approximation collapse points. Based on an idea that springs from [8], we propose an iterative extension to the standard random phase approximation method, which somewhat avoids a quasi-boson approximation. Lastly, in Chapter 4, the Bardeen-Cooper-Schrieffer method, which allows one to describe pairing interactions, is introduced and applied to the Lipkin model. We comment on similar works that applied the BCS method to this model in [17, 18].

In summary, we apply five many-body methods to the Lipkin model. These methods are the Hartree-Fock mean-field method, the random phase approximation, the Tamm-Dancoff approximation, the random phase iterative extension, and the Bardeen-Cooper-Schrieffer method. These approximate methods are used to find the best approximation for either the ground state energy or excited state energies. Throughout the thesis, we give many numerical comparisons of all these methods. As it was already done in [10, 11], we explore the energy approximations as functions of interactions strengths. To that, we add their relative errors with respect to exact solutions. On top of that, the performance of these approximations as a function of particle number is studied.

Chapter 1

# Nuclear Lipkin Model

1.1 The model & Exact solutions

To begin with, we give a brief introduction to the Lipkin model, which was originally intended as a testing ground for many-body methods [1–3]. In general, the system consists of two levels occupied by a total of N fermion-like particles, thus each level is N times degenerated. The two levels are separated by energy gap ε. In addition to that, the system is enhanced by two types of two-body interactions commonly denoted as V and W. The first interaction V takes a pair of two particles at either of the two levels and scatters it to the other level, while the interaction W simultaneously scatters a particle from the lower level to the upper one, and vice versa. To conceptually approach the model, we think of the system with both interactions disabled. This way, the ground state is realized by all particles occupying the lower shell only. Once a single particle is scattered to the upper level, we get the first excited state and so on, as depicted in Fig. 1.1.1.
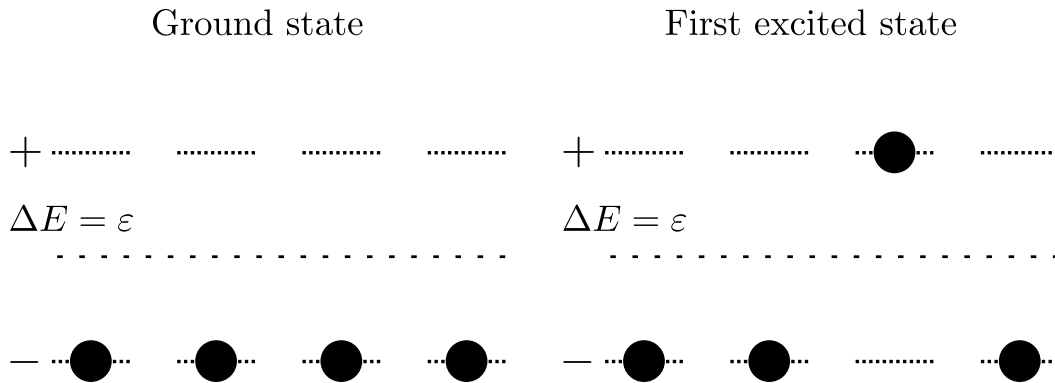
Figure 1.1.1 Scheme of two-level Lipkin model found in the ground state and in the first excited state with both interactions V and W disabled.

If one considers the non-interacting case, the model is trivial to solve. Once either interaction V or W is included, the problem immediately becomes more

involved. As we will see, it is especially interaction V that complicates it. Despite that, the model can still be largely simplified using internal symmetries, and in the case of pure interaction W, exact solutions can be obtained by hand. Suppose both interactions V and W are included. In that case, exact solutions are known only for a few special values of particle number N [19]. In Fig. 1.1.2, we give a graphical interpretation for both V and W interaction processes.
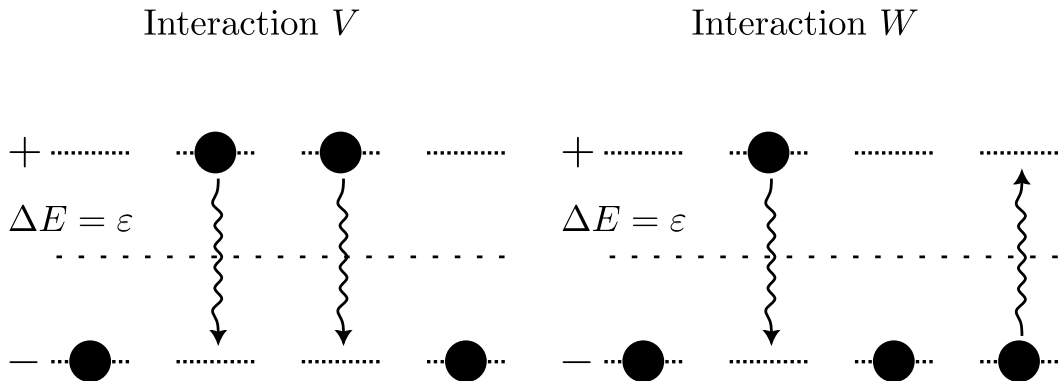
Figure 1.1.2 Scheme displaying interactions V and W in the two-level Lipkin model.

Let us introduce standard energy operator H [1] of the Lipkin model with the sign convention according to [10]. This Hamiltonian H that includes both interactions V and W reads

$$H = \frac{\varepsilon}{2} \sum_{n,\sigma}^{\Omega} \sigma a_{n\sigma}^\dagger a_{n\sigma} - \frac{V}{2} \sum_{n,m,\sigma}^{\Omega} a_{n\sigma}^\dagger a_{m\sigma}^\dagger a_{m-\sigma} a_{n-\sigma} - \frac{W}{2} \sum_{n,m,\sigma}^{\Omega} a_{n\sigma}^\dagger a_{m-\sigma}^\dagger a_{m\sigma} a_{n-\sigma},$$

$$(1.1.1)$$

where $\sigma = \pm$ represents the upper $(+)$ and the lower $(-)$ level of the system, V and W stand for the interaction strengths, ε is the energy gap between the two levels, Ω denotes the total capacity of each shell equal to the particle number N, which is just the total number of particles in the system, and $a_{k\sigma}^\dagger$ together with $a_{l\sigma}$, stand for the usual creation and annihilation fermionic operators [20, 21]. At this point, our goal is to solve for the stationary Schrödinger equation

$$H|\psi\rangle = E|\psi\rangle, \qquad (1.1.2)$$

namely, we want to find stationary energies E and corresponding stationary states $|\psi\rangle$. For a system defined by energy operator H in Eq. (1.1.1), a total of 2^N possible states exist, making it very difficult to solve Eq. (1.1.2) directly.

However, it turns out one can exploit an internal symmetry within the system

[1, 10] given by Eq. (1.1.1) and introduce the following operators

$$K_0 = \frac{1}{2} \sum_n^{\Omega} \left(a_{n+}^\dagger a_{n+} - a_{n-}^\dagger a_{n-} \right), \tag{1.1.3}$$

$$K_+ = \sum_n^{\Omega} a_{n+}^\dagger a_{n-}, \tag{1.1.4}$$

$$K_- = \sum_n^{\Omega} a_{n-}^\dagger a_{n+}, \tag{1.1.5}$$

$$K^2 = \frac{1}{2} \{K_+, K_-\} + K_0^2, \tag{1.1.6}$$

with $(K_+)^\dagger = K_-$. This way, Eq. (1.1.1) can thus be expressed as

$$H = \varepsilon K_0 - \frac{V}{2} \left(K_+^2 + K_-^2 \right) - \frac{W}{2} \left(K_+ K_- + K_- K_+ \right). \tag{1.1.7}$$

Operators K_0, $K_\pm$ and K^2 satisfy the very same commutation relations as the regular angular momentum operators [20, 21]

$$\begin{array}{ll}
[J_z, J^2] = 0, & [K_0, K^2] = 0, \quad (1.1.8) \\
[J_z, J_\pm] = \pm J_\pm, & [K_0, K_\pm] = \pm K_\pm, \quad (1.1.9) \\
[J_+, J_-] = 2 J_z, & [K_+, K_-] = 2 K_0. \quad (1.1.10)
\end{array}$$

The set of operators $\{K_0, K_\pm\}$ thus produces what is often referred to as the quasi-spin algebra. To prove this to be true, we set out to verify commutators in Eq. (1.1.8) to Eq. (1.1.10).

We start by computing the commutator in Eq. (1.1.9)

$$[K_0, K_+] =$$

$$= \frac{1}{2} \sum_{n,m}^{\Omega} \left[\left(a_{n+}^\dagger a_{n+} - a_{n-}^\dagger a_{n-} \right) a_{m+}^\dagger a_{m-} - a_{m+}^\dagger a_{m-} \left(a_{n+}^\dagger a_{n+} - a_{n-}^\dagger a_{n-} \right) \right] =$$

$$= \frac{1}{2} \sum_{n,m}^{\Omega} \left[a_{n+}^\dagger a_{n+} a_{m+}^\dagger a_{m-} - a_{n-}^\dagger a_{n-} a_{m+}^\dagger a_{m-} - a_{m+}^\dagger a_{m-} a_{n+}^\dagger a_{n+} + \right.$$

$$\left. + a_{m+}^\dagger a_{m-} a_{n-}^\dagger a_{n-} \right] = \frac{1}{2} \sum_{n,m}^{\Omega} \left[a_{n+}^\dagger a_{m-} \delta_{nm} \delta_{++} - a_{n+}^\dagger a_{m+}^\dagger a_{n+} a_{m-} - \right.$$

$$- a_{n-}^\dagger a_{m-} \delta_{nm} \delta_{-+} + a_{n-}^\dagger a_{m+}^\dagger a_{n-} a_{m-} - a_{m+}^\dagger a_{n+} \delta_{nm} \delta_{-+} + a_{m+}^\dagger a_{n+}^\dagger a_{m-} a_{n+} +$$

$$\left. + a_{m+}^\dagger a_{n-} \delta_{nm} \delta_{--} - a_{m+}^\dagger a_{n-}^\dagger a_{m-} a_{n-} \right] = \frac{1}{2} \sum_{n,m}^{\Omega} \left[a_{n+}^\dagger a_{m-} \delta_{nm} + \right.$$

$$\left. + a_{m+}^\dagger a_{n-} \delta_{nm} \right] = \sum_n^{\Omega} a_{n+}^\dagger a_{n-} = K_+.$$

$$\tag{1.1.11}$$

The other commutator $[K_0, K_+]$ is straightforward due to $(K_+)^\dagger = K_-$ property

$$K_- = (K_+)^\dagger = ([K_0, K_+])^\dagger = (K_0 K_+ - K_+ K_0)^\dagger = (K_+)^\dagger K_0 - K_0 (K_+)^\dagger =$$
$$= -(K_0 K_- - K_- K_0) = -[K_0, K_-],$$

(1.1.12)

with $K_0 = (K_0)^\dagger$ being just trivial.

Next, we check the commutation relation in Eq. (1.1.10)

$$[K_+, K_-] = K_+ K_- - K_- K_+ = \sum_{n,m}^{\Omega} \left(a_{n+}^\dagger a_{n-} a_{m-}^\dagger a_{m+} - a_{m-}^\dagger a_{m+} a_{n+}^\dagger a_{n-} \right) =$$

$$= \sum_{n,m}^{\Omega} \left(a_{n+}^\dagger a_{m+} \delta_{nm} \delta_{--} - a_{n+}^\dagger a_{m-}^\dagger a_{n-} a_{m+} - a_{m-}^\dagger a_{n+}^\dagger \delta_{nm} \delta_{++} + \right.$$

$$\left. + a_{m-}^\dagger a_{n+}^\dagger a_{m+} a_{n-} \right) = \sum_{n}^{\Omega} \left(a_{n+}^\dagger a_{n+} - a_{n-}^\dagger a_{n-} \right) = 2K_0.$$

(1.1.13)

At last, we want to show Eq. (1.1.8) also holds true

$$\left[K^2, K_0\right] = K^2 K_0 - K_0 K^2 = \frac{1}{2}\{K_+, K_-\} K_0 + K_0^3 - \frac{1}{2} K_0 \{K_+, K_-\} - K_0^3 =$$

$$= \frac{1}{2}\left(K_+ K_- K_0 + K_- K_+ K_0 - K_0 K_+ K_- - K_0 K_- K_+\right) = \frac{1}{2}\left(K_+ K_0 K_- + \right.$$

$$+ K_+ K_- - K_- K_+ + K_- K_0 K_+ - K_+ K_- - K_+ K_0 K_- + K_- K_+ + K_- K_0 K_+) =$$

$$= 0,$$

(1.1.14)

where the result of Eq. (1.1.11) was used to arrive at the third equality.

We proved that the set of operators $\{K_0, K_\pm\}$ follows the usual angular momentum commutation relations. This way, we can fully employ the angular momentum algebra machinery to solve the eigenvalue problem in Eq. (1.1.2) prescribed by the Hamiltonian operator H in Eq. (1.1.1).

Next, we realize that K^2 commutes with H

$$\left[H, K^2\right] = 0.$$

(1.1.15)

That is also easy to show that

$$\left[H, K^2\right] = \varepsilon \left[K_0, K^2\right] - \frac{V}{2}\left[K_+^2, K^2\right] - \frac{V}{2}\left[K_-^2, K^2\right] - \frac{W}{2}\left[K_+ K_-, K^2\right] -$$

$$- \frac{W}{2}\left[K_- K_+, K^2\right] = -\frac{V}{2}\left(K_+^2 K^2 - K^2 K_+^2 - K_-^2 K^2 + K^2 K_-^2\right) -$$

$$- \frac{W}{2}\left(K_+ K_- K^2 - K^2 K_+ K_- + K_- K_+ K^2 - K^2 K_- K_+\right) =$$

$$= -\frac{V}{2}\left(K^2 - K_0^2\right) K^2 - \frac{V}{2} K_0^2 \left(-K^2 + K_0^2\right) -$$

$$- \frac{W}{2}\left(K_+ K_- + K_- K_+\right) K^2 + \frac{W}{2} K^2 \left(K_- K_+ + K_+ K_-\right) =$$

$$= 0 - W\left(K^2 - K_0^2\right) K^2 + W K^2 (K^2 - K_0^2) = 0.$$

(1.1.16)

So far, we defined operators K_0 and $K_\pm$, which satisfy the usual angular momentum algebra. In Eq. (1.1.7), we then expressed energy operator H from Eq. (1.1.1) in terms of these operators. This makes the original problem from Eq. (1.1.2) nearly trivial. If we let $|k, m\rangle$ be a basis for the quasi-spin operators, we get the usual action of K^2, K_0, and $K_\pm$ operators

$$K_0|k, m\rangle = m\,|k, m\rangle, \tag{1.1.17}$$

$$K^2|k, m\rangle = k(k + 1)\,|k, m\rangle, \tag{1.1.18}$$

$$K_\pm|k, m\rangle = \sqrt{k(k \pm 1) - m(m \pm 1)}|k, m \pm 1\rangle. \tag{1.1.19}$$

Eq. (1.1.17) to Eq. (1.1.19) follow from the angular momentum algebra.

In particular, the quantum numbers k and m take the values

$$k = \frac{N}{2}, \tag{1.1.20}$$

$$m = -\frac{N}{2}, -\frac{N}{2} + 1, \ldots, \frac{N}{2}, \tag{1.1.21}$$

quantum number k is thus fixed by the particle number N, which just gives the total number of particles in the system. In contrast, the other quantum number m just follows from Eq. (1.1.3) and corresponds to the difference of particle numbers N_- and N_+ each giving the number of particles occupying either the lower or the upper shell.

To appreciate what was achieved to this point, one just compares the dimension of the matrix representing H in Eq. (1.1.1) whose dimension was $2^N \times 2^N$ to that in Eq. (1.1.7) with the size of $(N + 1) \times (N + 1)$. This is an incredible reduction of work, especially for large values of N, not to mention it is easier to work with K_0 and $K_\pm$ operators in the first place.

Solving the original problem in Eq. (1.1.2) thus reduces to writing down H matrix in $|k, m\rangle$ basis and computing its eigenvalues and eigenvectors. In principle, this is always possible, either by numerical means or by applying various many-body approximate methods.

To get an idea of how spectra of the operator H in Eq. (1.1.1) look like, in Fig. 1.1.3 we plot the whole spectrum of the Lipkin model for several systems with different values of particle number N and different interactions strengths V and W. Right now we postpone the discussion of the spectra and somewhat intriguing phenomena within them to the next Section 1.1.

Before we proceed any further, we also introduce reduced interaction strengths[1] v and w parameters for interactions V and W respectively

$$v = V\frac{(N - 1)}{\varepsilon}, \tag{1.1.22}$$

$$w = W\frac{(N - 1)}{\varepsilon}. \tag{1.1.23}$$

As of right now, the definition in Eq. (1.1.22) and Eq. (1.1.23) may seem odd, and in fact, it is, but as we will see, it makes the problem somewhat easier to deal with once approximate methods are employed. At the same time, the definition in Eq. (1.1.22) and Eq. (1.1.23) makes the interaction strengths independent of particle number N, which turns out to be quite handsome.

---

[1]For the sake of brevity, we also refer to both v and w as just interaction strengths.
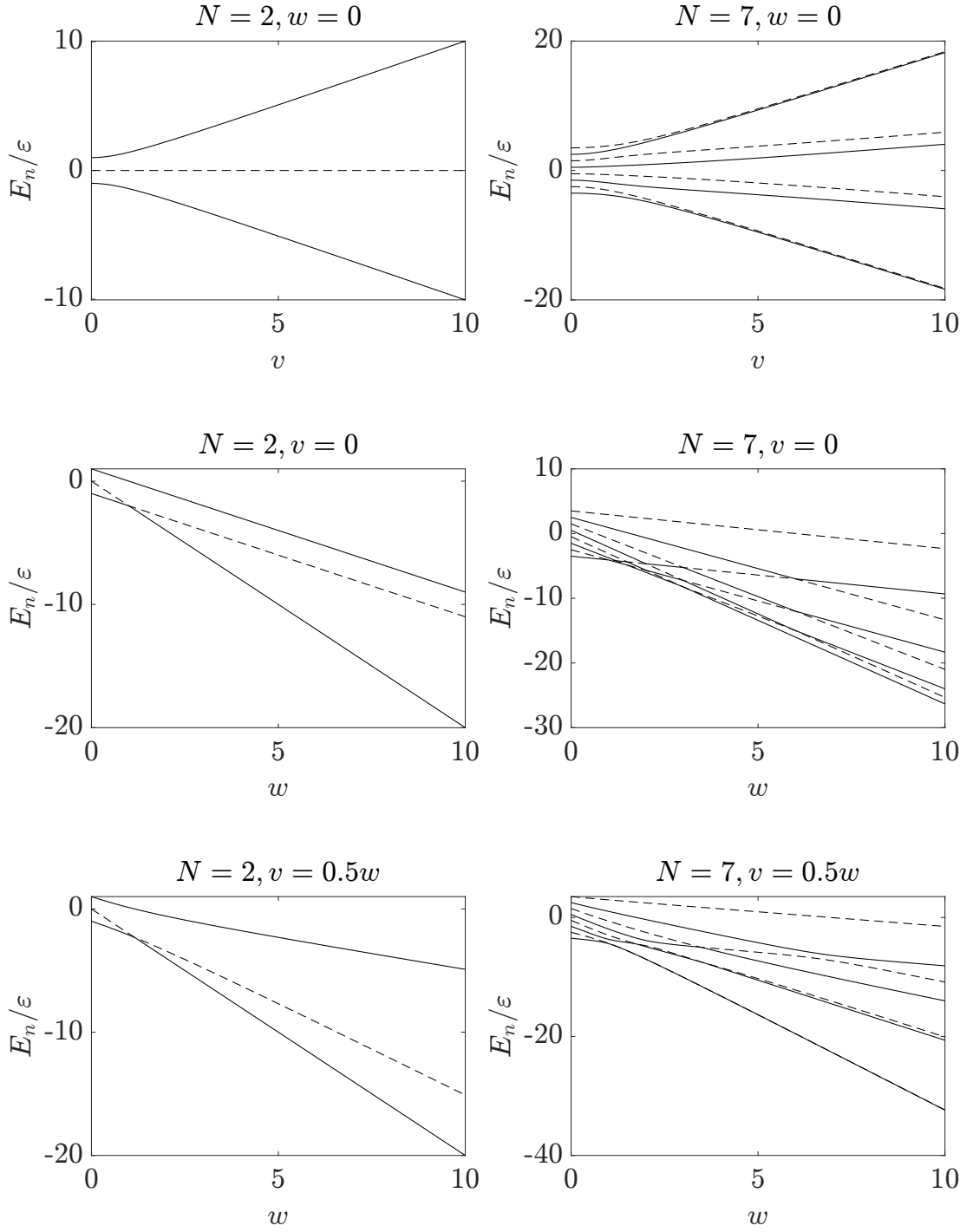
Figure 1.1.3 Relative eigenenergies E_n/ε for the Lipkin model given by H in Eq. (1.1.1) for different values of particle number N and different v and w interaction strengths as functions of either v or w. To distinguish between two subsequent spectral lines, we keep switching between solid lines and dashed lines.

1.2 Physical content of the solutions

Previous Section 1.1 introduced the Lipkin model. We then exploited an internal symmetry of the model, which made it possible to either directly solve the eigenvalue problem in Eq. (1.1.2) or largely simplify it if interaction V was present. Nonetheless, little was said of any actual physical content of the solutions. In what follows in Chapter 2 to Chapter 4, we will directly encounter some of the physical features. Because of that, we show what some of these features are and how they appear in the exact solutions.

Spectrum properties & Phase transitions

To begin with, we return to a discussion regarding the spectra in Fig. 1.1.3. We see that the spectrum tends to be symmetric by setting $w = 0$ and letting $E_n(v)$ be a function of v. Also, in the limit $v \to +\infty$, the spectral lines tend to further degenerate, which is well seen in the case of $N = 7$ particles. To understand this, we realize that interaction V scatters a pair of particles from one level to the other. This way, if V is large, the total effective number of particles reduces by half due to the action of the interaction, hence the spectrum tends to degenerate.

In contrast, the interaction W does precisely the opposite; in some sense, it removes the symmetry, and on top of that, it also causes the spectral lines to intersect. This is best seen in the case when $v = 0$. If we were to track down the ground state spectral lines, at the point of intersection we learn that the derivatives of E_0 are ill-defined. In fact, at points such as these, a phase transition (PT) takes place. In the context of the Lipkin model, the PTs are well-known phenomena [5, 7] and a lot of literature is explicitly dedicated to the study of PTs within this particular model. To put this in a different perspective, in Fig. 1.2.1, we plot the probability amplitudes of measuring the first three stationary energies E_0, E_1 and E_2 for a system initially prepared in state $|\psi\rangle = |k, -k\rangle$, where $k = N/2$, which gives the ground state when $v = w = 0$. At the point $w = 1$, we see that for both systems with $N = 2$ and $N = 7$, a non-continuous change in probability amplitude occurs, thus also implying the system undergoes a PT at this point.

For a system with pure interaction W, the existence of a PT can be shown by analytic means. Setting $V = 0$ Eq. (1.1.7) reads

$$H = \varepsilon K_0 - \frac{W}{2}\left(K_+ K_- + K_- K_+\right). \tag{1.2.1}$$

In particular, H is a diagonal matrix with the diagonal elements being given by

$$H_{mm} = \langle k, m|H|k, m\rangle = m\varepsilon - W\left[k(k+1) - m^2\right], \tag{1.2.2}$$

which is due to the anti-commutator $\{K_+, K_-\}$ action on $|k, m\rangle$ (for details see Appendix A).

To show the existence of the first PT in the ground state energy E_0, we take the two elements of H, which belong to the two lowest values of m

$$E(m = -\frac{N}{2}) = -\varepsilon\left(\frac{N}{2} + \frac{N}{2(N-1)}w\right), \tag{1.2.3}$$

$$E(m = -\frac{N}{2} + 1) = -\varepsilon\left(\frac{N-1}{2} + \frac{3N-2}{2(N-1)}w\right). \tag{1.2.4}$$

For $w < 1$, we see that $E(m = -\frac{N}{2})$ gives the lowest energy and thus corresponds to the ground state. However, if $w > 1$, this is no longer true, and it is $E(m = -\frac{N}{2}+1)$ which gives lower energy than $E(m = -\frac{N}{2})$, and hence gives the ground-state energy. At the points of intersection with $w = 1$ the two energies $E(m = -\frac{N}{2})$ and $E(m = -\frac{N}{2} + 1)$ are equal.

On top of that, first derivatives with respect to reduced interaction strength w are not equal for $w = 1$, that is

$$\frac{\mathrm{d}E(m = -\frac{N}{2})}{\mathrm{d}w} \neq \frac{\mathrm{d}E(m = -\frac{N}{2} + 1)}{\mathrm{d}w}. \tag{1.2.5}$$

We see that at a point where $w = 1$, the system will always undergo a PT in its ground state. In principle, the same analysis could be done for all the other PTs in the model.
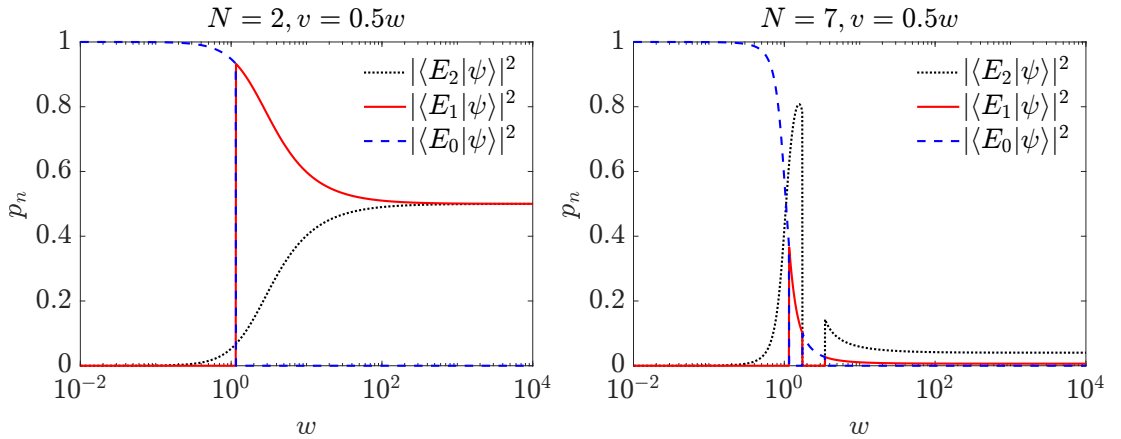
Figure 1.2.1 Probability amplitudes $p_n = |\langle E_n|\psi\rangle|^2$ of finding the system prepared in the initial state $|\psi\rangle = |k, -k\rangle$, $k = N/2$ with energy E_n as a function of interaction strength w.

Odd-even effect analogy

So-called odd-even effect [8] is a fascinating phenomenon observed in nuclei. Suppose one were to track the binding energies of nuclei. In that case, it turns out that the binding energy of an odd-even nucleus is smaller than the arithmetic mean of binding energies of two even-even nuclei, the first with one more nucleon and the second with one nucleon less. This effect is caused by a pairing interaction between nucleons in the nuclei as explained in [8]. Simply put, a many-body system with all its particles paired will have higher binding energy than an equivalent system without this type of interaction.

An analogy to this particular effect can be observed in the Lipkin model. This is due to interaction W, which is an example of a pairing interaction. Essentially, the interaction W pairs two particles, each sitting at a different level. To show this, we limit ourselves to a system with interaction W only. Eigenenergies of such system follow from Eq. (1.2.2).

12

To begin with, we let $0 < w < 1$. Under these circumstances, the odd-even-like effect is given by the following inequality

$$E_0(N) \geq \frac{1}{2} \left[E_0(N+1) + E_0(N-1) \right]. \tag{1.2.6}$$

To show inequality in Eq. (1.2.6) to be true, we just substitute $E_0(N) = -\varepsilon \left(\frac{N}{2} + \frac{N}{2(N-1)} w \right)$, which comes from Eq. (1.2.3). This brings us to

$$-\varepsilon \frac{N}{2} \left(\frac{1}{2} + \frac{w}{N-1} \right) \geq -\varepsilon \frac{N}{4} \left(1 + \frac{w}{N} + \frac{w}{N-2} \right), \tag{1.2.7}$$

which is trivially true. In fact, the odd-even effect analogy will always appear in the Lipkin model when $0 < w < 1$ and $v = 0$. However, if one let $w > 1$, the odd-even effect may be broken because Eq. (1.2.6) will not be true in general. This is caused by phase transitions which lead to a change in the ground state energy.

To better visualise this, in Fig. 1.2.2 we plot relative binding energy difference $\Delta B(N)/\varepsilon$, with binding energy difference $\Delta B(N)$ defined as

$$\Delta B(N) = \frac{1}{2} \left[E_0(N+1) + E_0(N-1) \right] - E_0(N), \tag{1.2.8}$$

for odd values of N. When $w = 0.8$, we see an odd-even effect analogy in the system, the effect disappears for $w = 5$ when $v \neq 0$. In Fig. 1.2.2, we also notice that interaction v does not break the odd-even effect and even causes it to restore for large values of w. Unfortunately, making a general analysis with v included is hard for an arbitrary value of N.
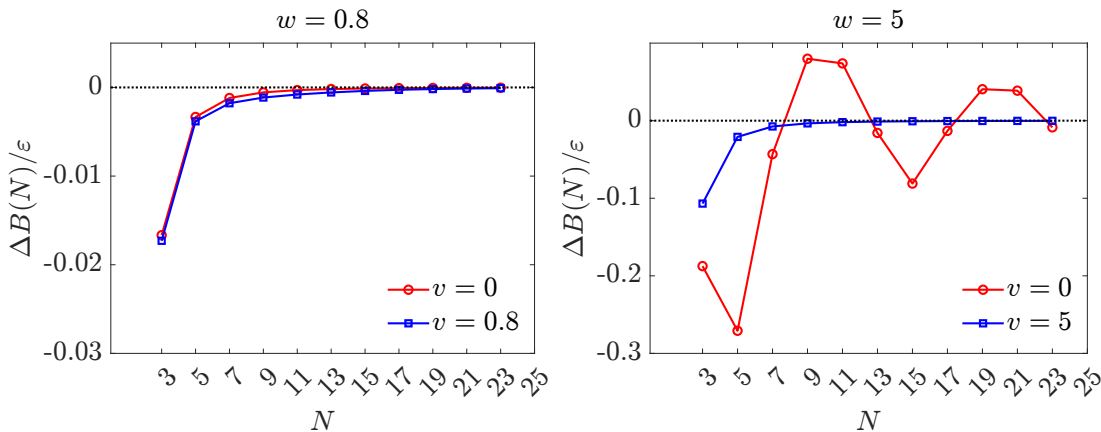
Figure 1.2.2 Plot of relative binding energy difference $\Delta B(N)/\varepsilon$ as a function of particle number N starting at $N_0 = 3$ for odd values of N, for given values of interaction strengths v and w.

Chapter 2

Hartree-Fock Method

2.1 Why mean-field?

Before we get straight into the Hartree-Fock mean-field theory and its application to the Lipkin model, we list a few reasons to justify mean-field as a reasonable way to solve a many-body problem in quantum mechanics.

To get things going, let us suppose we had an arbitrary quantum system composed of N indistinguishable particles. This system may be an atom or a nucleus. Just as in [8], we assume the following two conditions to be true.

- Velocity of each individual particle in the system is small $1 \gg v^2/c^2$ so that non-relativistic quantum mechanics provides a suitable description for the system.

- There are only two-body interactions between the particles in the system, and if not, we assume any multi-body interactions of higher order to be negligible with respect to the two-body interactions.

In the coordinate representation, we may write a corresponding time-independent Schrödinger equation for a given system as

$$H\Psi = \left[\sum_n \left(-\frac{\hbar^2}{2m_n}\nabla_n^2\right) + \frac{1}{2}\sum_{n \neq m} V(n,m)\right]\Psi = E\Psi, \qquad (2.1.1)$$

with H being the appropriate energy operator of the system, $V(n,m)$ being a two-body interaction potential operator, m_n being mass of nth particle and Ψ is denoting a wave function.

In general, solving Eq. (2.1.1) can be extremely difficult. In order to do that, one often has to seek out a way to approximate the problem in Eq. (2.1.1). One particular way to achieve this as proposed in [8, 17] is to replace H energy operator with a new Hamiltonian H_0 that gives a one-body approximation of H

$$H_0\Psi = \sum_n \left[-\frac{\hbar^2}{2m_n}\nabla_n^2 + \widetilde{V}(n)\right]\Psi = \varepsilon\Psi. \qquad (2.1.2)$$

Here $\widetilde{V}(n)$ stands for a new effective one-body interaction potential that optimally approximates the original two-body potential $V(n,m)$.

The eigenstates corresponding to $\widetilde{V}$ then provide a one-particle state basis for a variational space that is used to approximately solve the original eigenvalue problem in Eq. (2.1.1).

The procedure sketched above is in fact the core idea behind the Hartree-Fock mean-field method [8]. In a nutshell, one takes an arbitrary multi-body interaction potential V and replaces it with an effective one-body interaction potential $\widetilde{V}$. As soon as an appropriate $\widetilde{V}$ is found, one then derives Hartree-Fock equations [8], and tries to solve them. The Hartree-Fock equations represent a significantly easier eigenvalue problem for the one-body Hamiltonian H_0. If one aspires to look for the ground state energy only, it is sufficient to minimize the usual energy functional as in detail discussed in [8, 20, 21], with the test-function space spanned by elements of the Hartree-Fock mean-field basis. This of course is just an approximation. However, it turns out to work very well if the residual interaction $V_{\mathrm{Res}} \equiv (V - \widetilde{V})$ is small. In Section 2.2 we give a more formal treatment of the Hartree-Fock mean-field method and in Section 2.3 we apply it to the Lipkin model.

2.2 Hartree-Fock method & Variational principles

Before we turn our attention to the Hartre-Fock (HF) mean-field method, we first recall some of the most important results concerning the variational principles in quantum mechanics.

Starting with the Ritz Principle as in [8, 20, 21]

$$H|\phi\rangle = E|\phi\rangle \qquad \Longleftrightarrow \qquad \delta E\left[|\phi\rangle\right] = 0, \tag{2.2.1}$$

with the energy functional $E\left[|\psi\rangle\right]$ given as

$$E\left[|\phi\rangle\right] = \frac{\langle\phi|H|\phi\rangle}{\langle\phi|\phi\rangle}, \tag{2.2.2}$$

and an arbitrary state $|\phi\rangle \in \mathcal{H}$ from an appropriate Hilbert space $\mathcal{H}$. Let E_0 be the exact ground state energy of the problem in Eq. (2.2.1). For $E\left[|\phi\rangle\right]$ it then holds that

$$E\left[|\phi\rangle\right] = \frac{\sum\limits_{n,m} c_n c_m^* E_n \delta_{nm}}{\sum\limits_{n} |c_n|^2} \geq \frac{\sum\limits_{n} |c_n|^2 E_0}{\sum\limits_{n} |c_n|^2} = E_0, \tag{2.2.3}$$

where $|\phi\rangle \in \mathcal{H}$ is expanded in a basis $\{|\psi_n\rangle\}_n$ of $\mathcal{H}$ as

$$|\phi\rangle = \sum_n c_n|\psi_n\rangle. \tag{2.2.4}$$

Now we finally get to the HF method. Let us assume it is possible to approximate the energy operator H of the original problem with a one-body Hamiltonian H_0

$$H \approx H_0 = \sum_n h_n. \tag{2.2.5}$$

In many cases, approximation from Eq. (2.2.5) is feasible. A procedure to reduce an arbitrary two-body Hamiltonian H to a corresponding one-body Hamiltonian H_0 is shown in [17].

Next, we construct the HF ground state $|HF\rangle$. We assume the ground state to be of a general one-particle product form

$$|HF\rangle = |\Phi\rangle = \prod_n a_n^\dagger |0\rangle, \qquad (2.2.6)$$

with $|0\rangle$ being the vacuum state and $a_n^\dagger$ being corresponding fermion particle creation operators. Wave function $|\Phi\rangle$ in Eq. (2.2.6) is a Slater determinant [8], made out of one-particle wave functions ϕ_n which satisfy the one-body problem

$$h_n \phi_n = E_n \phi_n. \qquad (2.2.7)$$

We return to the original problem given by Hamiltonian H. An arbitrary energy operator H can be expressed in terms of creation and annihilation operators $c_k^\dagger$ and c_l, it can be expanded as [8]

$$H = \sum_{k,l} T_{kl} c_k^\dagger c_l + \frac{1}{4} \sum_{k,l,m,n} \overline{V}_{klmn} c_k^\dagger c_l^\dagger c_n c_m, \qquad (2.2.8)$$

where T_{kl} and $\overline{V}_{klmn}$ are matrix elements of a one-body kinetic energy operator T and an antisymmetric two-body potential energy operator $\overline{V}$.

The point now is to find some appropriate unitary transform U

$$U^\dagger U = U U^\dagger = I, \qquad (2.2.9)$$

so that the set of $c_n^\dagger$ and c_n operators of the exact many-body problem is transformed to the set of $a_m^\dagger$ and a_m operators which correspond to the reduced one-body interaction problem given in Eq. (2.2.5)

$$a_m^\dagger = \sum_n U_{mn} c_n^\dagger. \qquad (2.2.10)$$

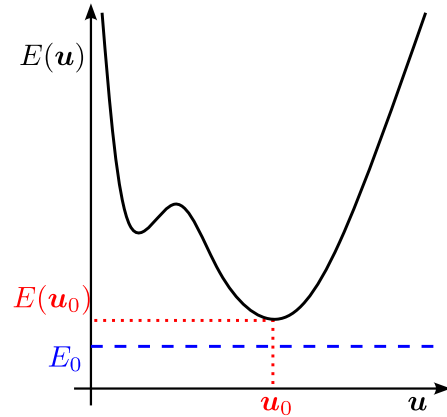Simultaneously, wave functions ϕ_n are also transformed by U as

$$\phi_m = \sum_n U_{mn} \varphi_n, \qquad (2.2.11)$$

with $\{\varphi_n\}_n \subset \mathcal{H}$ being a subset of $\mathcal{H}$ Hilbert space of exact problem given by H. Note that if $\{\phi_m\}_m$ is an orthonormal set of functions, due to the unitarity of U, $\{\varphi_n\}_n$ is also an orthonormal set of functions.

Figure 2.2.1 Variational ground state energy approximation $E_{(}\boldsymbol{u}_0)$ gives an upper bound to the exact E_0 energy.

Finally, we deploy the variational principles [8] and define the HF ground state energy approximation as

$$E_0^{\mathrm{HF}}(\boldsymbol{u}) = \langle HF(\boldsymbol{u})|H|HF(\boldsymbol{u})\rangle. \qquad (2.2.12)$$

Eq. (2.2.12) is just the energy functional of H evaluated at $|HF\rangle$. The point of the HF method now is to find such $|HF\rangle$ mean-field ground state that minimizes $E_0^{\mathrm{HF}}(\boldsymbol{u})$ with respect to the variational parameter $\boldsymbol{u}$, which comes from the U transform. For $\boldsymbol{u} = \boldsymbol{u}_0$ that makes $E_0^{\mathrm{HF}}(\boldsymbol{u})$ the lowest, corresponding $|HF(\boldsymbol{u}_0)\rangle$ defines the HF mean-field ground state and gives the corresponding HF mean-field ground state energy $E_0^{\mathrm{HF}}(\boldsymbol{u}_0)$.

2.3 Mean field solution of the Lipkin model

We apply now the HF method to the Lipkin model. First, we seek to find a unitary transformation U, which transforms the original many-body problem to a one-body counterpart, such that the total ground state mean energy is minimal. In the context of the Lipkin model, HF approximation was already studied earlier in [8, 10, 11]. The main goal of this section is to verify results from [10, 11], which will be subsequently further elaborated upon in Chapter 3 and to some extent in Chapter 4.

To start off, we introduce an arbitrary unitary transformation of creation and annihilation operators for both levels as

$$\begin{pmatrix} \widetilde{a}_{n+}^\dagger \\ \widetilde{a}_{n-}^\dagger \end{pmatrix} = \begin{pmatrix} \cos(\beta) & -\sin(\beta) \\ \sin(\beta) & \cos(\beta) \end{pmatrix} \begin{pmatrix} a_{n+}^\dagger \\ a_{n-}^\dagger \end{pmatrix}, \tag{2.3.1}$$

which produces a transformation from the original $|k, m\rangle$ basis to a new mean-field basis $|\widetilde{k}, \widetilde{m}\rangle$, with $\beta \in [0, 2\pi]$. Also note that, the transformed creation and annihilation operators $\widetilde{a}_{n\pm}^\dagger$ and $\widetilde{a}_{n\pm}$ still do satisfy the anti-commutation relations for fermions.

This way, one can also transform K_0 and $K_\pm$ operators to the new basis. The transformation is given by some 3×3 transformation matrix O

$$\begin{pmatrix} K_+ \\ K_0 \\ K_- \end{pmatrix} = O \begin{pmatrix} \widetilde{K}_+ \\ \widetilde{K}_0 \\ \widetilde{K}_- \end{pmatrix}. \tag{2.3.2}$$

The idea now is to find this particular transformation O from Eq. (2.3.2) and rewrite the original Hamiltonian H in Eq. (1.1.7) using the transformed operators $\widetilde{K}_0$ and $\widetilde{K}_\pm$. To make things clear, in the new basis $|\widetilde{k}, \widetilde{m}\rangle$ we shall refer to the transformed Hamiltonian H as $\widetilde{H}$.

Using the transformation definition in Eq. (2.3.1), for K_0 one gets

$$K_0 = \cos(2\beta)\widetilde{K}_0 + \frac{1}{2}\sin(2\beta)\left[\widetilde{K}_+ + \widetilde{K}_-\right]. \tag{2.3.3}$$

Similarly for $K_\pm$ we obtain

$$K_+ = \cos^2(\beta)\widetilde{K}_+ - \sin^2(\beta)\widetilde{K}_- + \sin(2\beta)\widetilde{K}_0, \tag{2.3.4}$$

$$K_- = \cos^2(\beta)\widetilde{K}_- - \sin^2(\beta)\widetilde{K}_+ + \sin(2\beta)\widetilde{K}_0. \tag{2.3.5}$$

Details concerning the derivation of Eq. (2.3.3) to Eq. (2.3.5) are to be found in Appendix A.

Therefore we express Eq. (2.3.2) as

$$\begin{pmatrix} K_+ \\ K_0 \\ K_- \end{pmatrix} = \frac{1}{2} \begin{pmatrix} 2\cos^2(\beta) & 2\sin(2\beta) & -2\sin^2(\beta) \\ \sin(2\beta) & 2\cos(2\beta) & \sin(2\beta) \\ -2\sin^2(\beta) & 2\sin(2\beta) & 2\cos^2(\beta) \end{pmatrix} \begin{pmatrix} \widetilde{K}_+ \\ \widetilde{K}_0 \\ \widetilde{K}_- \end{pmatrix}. \tag{2.3.6}$$

If we define $\alpha \equiv 2\beta$, using standard trigonometric identities, Eq. (2.3.6) can be recast into the following form

$$
\begin{pmatrix} K_+ \\ K_0 \\ K_- \end{pmatrix} = \frac{1}{2} \begin{pmatrix} \cos(\alpha)+1 & 2\sin(\alpha) & \cos(\alpha)-1 \\ \sin(\alpha) & 2\cos(\alpha) & \sin(\alpha) \\ \cos(\alpha)-1 & 2\sin(\alpha) & \cos(\alpha)+1 \end{pmatrix} \begin{pmatrix} \widetilde{K}_+ \\ \widetilde{K}_0 \\ \widetilde{K}_- \end{pmatrix}, \tag{2.3.7}
$$

which is a result that checks with that in [10, 11].

Now we find the form of $\widetilde{H}$ expressed in $|\widetilde{k}, \widetilde{m}\rangle$ basis. To this end, we have to substitute into K_0, $K_\pm^2$, and $K_\pm K_\mp$ terms in Eq. (1.1.7). This turns out to be a particularly tedious algebra exercise. In what follows, we give the results of each intermediate step (details covering the calculations are given in Appendix A).

In the case of interaction W sum term $K_+K_- + K_-K_+$ the result is

$$
K_+K_- + K_-K_+ = \frac{1}{2}\left(\cos^2(\alpha)-1\right)\left(\widetilde{K}_+^2 + \widetilde{K}_-^2\right) + 2\sin^2(\alpha)\widetilde{K}_0^2+
$$
$$
+ \frac{1}{2}\left(\cos^2(\alpha)+1\right)\left\{\widetilde{K}_+, \widetilde{K}_-\right\} + \sin(\alpha)\cos(\alpha)\left[\left\{\widetilde{K}_+, \widetilde{K}_0\right\} + \left\{\widetilde{K}_-, \widetilde{K}_0\right\}\right]. \tag{2.3.8}
$$

The other interaction V sum term $K_+^2 + K_-^2$ turns out to be

$$
K_+^2 + K_-^2 = \frac{1}{2}\left(\cos^2(\alpha)+1\right)\left(\widetilde{K}_+^2 + \widetilde{K}_-^2\right) + 2\sin^2(\alpha)\widetilde{K}_0^2+
$$
$$
+ \frac{1}{2}\left(\cos^2(\alpha)-1\right)\left\{\widetilde{K}_+, \widetilde{K}_-\right\} + 4\sin(\alpha)\cos(\alpha)\left[\left\{\widetilde{K}_-, \widetilde{K}_0\right\} + \left\{\widetilde{K}_+, \widetilde{K}_0\right\}\right]. \tag{2.3.9}
$$

Finally, substituting all preceding terms to Eq. (1.1.7) we write $\widetilde{H}$

$$
\widetilde{H} = \frac{\varepsilon}{2}\left[\sin(\alpha)\left(\widetilde{K}_+ + \widetilde{K}_-\right) + 2\cos(\alpha)\widetilde{K}_0\right] - \frac{W+V}{4}\left[\left(1+\cos^2(\alpha)\right)\cdot\right.
$$
$$
\left.\cdot\left(\widetilde{K}_+^2 + \widetilde{K}_-^2\right) - \sin(2\alpha)\left(\left\{\widetilde{K}_+, \widetilde{K}_0\right\} + \left\{\widetilde{K}_-, \widetilde{K}_0\right\}\right) + \right. \tag{2.3.10}
$$
$$
\left. + \sin^2(\alpha)\left(4\widetilde{K}_0^2 - \left\{\widetilde{K}_+, \widetilde{K}_-\right\}\right)\right] + \frac{W}{2}\left[\widetilde{K}_+^2 + \widetilde{K}_-^2 - \left\{\widetilde{K}_+, \widetilde{K}_-\right\}\right].
$$

As before, Eq. (2.3.10) is in agreement with both [10, 11].

At this point, we are nearly done. The task now is to use the variational principles, namely the one regarding the energy functional, and to minimize the total mean ground state energy with respect to the HF ground state.

To do this, we realize the action of $\widetilde{K}_0$ and $\widetilde{K}_\pm$ operators in $|\widetilde{k}, \widetilde{m}\rangle$ basis to be same to that of K_0 and $K_\pm$ in the original $|k, m\rangle$ basis

$$
\widetilde{K}_0|\widetilde{k}, \widetilde{m}\rangle = \widetilde{m}|\widetilde{k}, \widetilde{m}\rangle, \tag{2.3.11}
$$
$$
\widetilde{K}_\pm|\widetilde{k}, \widetilde{m}\rangle = \sqrt{(\widetilde{k} \mp \widetilde{m})(\widetilde{k} \pm \widetilde{m} + 1)}|\widetilde{k}, \widetilde{m} \pm 1\rangle. \tag{2.3.12}
$$

From the angular momentum algebra it then follows that

$$
\widetilde{K}_\pm^n|\widetilde{k}, \widetilde{m}\rangle \sim |\widetilde{k}, \widetilde{m} \pm n\rangle,
$$
$$
\{\widetilde{K}_\pm, \widetilde{K}_0\}|\widetilde{k}, \widetilde{m}\rangle \sim |\widetilde{k}, \widetilde{m} \pm 1\rangle.
$$

At this point, we also remind ourselves that $|\widetilde{k}, \widetilde{m}\rangle$ is an orthonormal basis

$$\langle \widetilde{k}, \widetilde{m}|\widetilde{k}', \widetilde{m}'\rangle = \delta_{\widetilde{k}\widetilde{k}'} \, \delta_{\widetilde{m}\widetilde{m}'}.$$

For simplicity, we denote the HF ground state as $|\widetilde{k}, -\widetilde{k}\rangle \equiv |HF\rangle$. From Eq. (2.3.10) we see that non-trivial contributions to $\langle HF|\widetilde{H}|HF\rangle$ matrix element stem from

$$\langle HF|\widetilde{K}_0|HF\rangle = -\frac{N}{2}, \tag{2.3.13}$$

$$\langle HF| \left\{ \widetilde{K}_+, \widetilde{K}_- \right\} |HF\rangle = N. \tag{2.3.14}$$

Eq. (2.3.13) is trivial and follows from Eq. (2.3.11), and Eq. (2.3.14) is also trivial due to the very same anti-commutator being already evaluated in Section 1.1 (details are given in Appendix A).

If we substitute the result from Eq. (2.3.13) and Eq. (2.3.14) back in Eq. (2.3.10) and make use of the energy functional in Eq. (2.2.12), all the non-zero $|HF\rangle$ ground state contributions just reduce down to

$$E_0^{HF}(\alpha) = -\frac{\varepsilon N}{2} \left[\cos(\alpha) + \frac{W}{\varepsilon} + \frac{(W+V)}{2\varepsilon}(N-1)\sin^2(\alpha) \right], \tag{2.3.15}$$

with $\alpha \in [-\pi, \pi]$ being the variational parameter. To give an idea of what the variational space of α parameter looks like, in Fig. 2.3.1 we plot $E_0^{HF}(\alpha)$ as a function of α for fixed particle number $N = 20$ and different values of v and w.
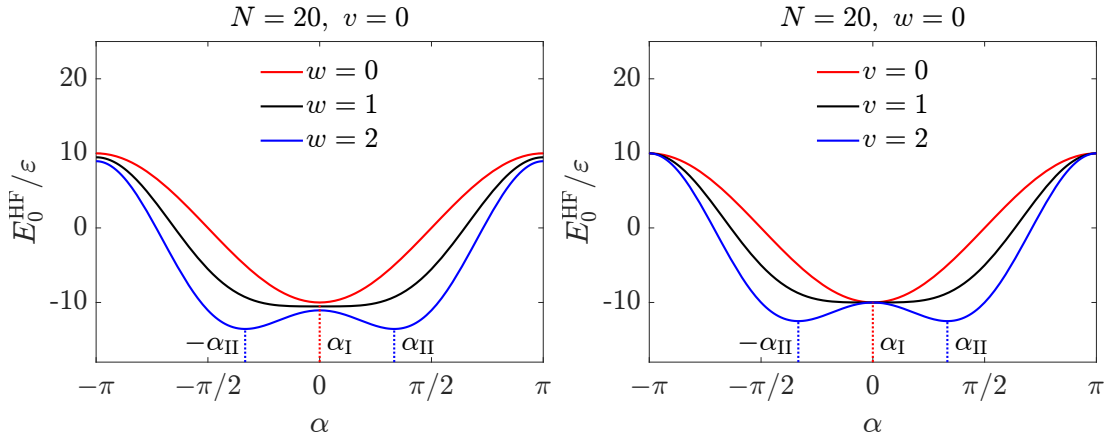
Figure 2.3.1 The HF ground state energy $E_0^{HF}(\alpha)/\varepsilon$ plot as a function of α parameter according to Eq. (2.3.16), with fixed particle number $N = 20$ and fixed interaction strengths v and w. Global minima points α_I are α_{II} are visualised by the dotted lines.

Going onwards, we minimise $E_0^{HF}(\alpha)$ with respect to α, more precisely we solve equation

$$\frac{dE_0^{HF}}{d\alpha}(\alpha) = \frac{\varepsilon N}{2}\sin(\alpha)\left[1 - \frac{(W+V)(N-1)}{\varepsilon}\cos(\alpha)\right] = 0. \tag{2.3.16}$$

Eq. (2.3.16) yields two possible extrema α_I and α_{II}

$$\alpha_I = 0, \qquad \alpha_{II} = \arccos\left(\frac{\varepsilon}{(N-1)(W+V)}\right). \tag{2.3.17}$$

Their corresponding ground state energies $E_0^{\text{HF}}(\alpha_{\text{I}})$ and $E_0^{\text{HF}}(\alpha_{\text{II}})$ are given by

$$E_0^{\text{HF}}(\alpha_{\text{I}}) = -\frac{N(\varepsilon + W)}{2}, \tag{2.3.18}$$

$$E_0^{\text{HF}}(\alpha_{\text{II}}) = -\frac{N}{4}\left[2W + \frac{\varepsilon^2 + (N-1)^2(V+W)^2}{(N-1)(V+W)}\right]. \tag{2.3.19}$$

Since $-1 \leq \cos(x) \leq 1$ with $x \in \mathbb{R}$, we immediately see the solution in Eq. (2.3.19) exists if and only if

$$1 \leq \left|\frac{\varepsilon}{(N-1)(W+V)}\right| = \left|\frac{1}{v+w}\right|, \tag{2.3.20}$$

with v and w being the reduced interaction strengths defined in Eq. (1.1.22) and Eq. (1.1.23). Let us decide which one of the two $E_0^{\text{HF}}(\alpha_{\text{I}})$ and $E_0^{\text{HF}}(\alpha_{\text{II}})$ solutions is the correct one for $v + w \geq 1$.

If we substitute v and w back to Eq. (2.3.18) and Eq. (2.3.19) and manipulate the terms a bit, it is easy to see the following inequality holds true

$$-\varepsilon\frac{N}{2}\left(1 + \frac{w}{N-1}\right) = E_0^{\text{HF}}(\alpha_{\text{I}}) \geq -\varepsilon\frac{N}{4}\left[\frac{2w}{N-1} + \frac{1+(v+w)^2}{v+w}\right] =$$
$$= E_0^{\text{HF}}(\alpha_{\text{I}}) - \varepsilon\frac{N[1+(v+w)^2]}{4(v+w)} = E_0^{\text{HF}}(\alpha_{\text{II}}). \tag{2.3.21}$$

Eq. (2.3.21) implies that if $v + w < 1$, the proper HF mean-field ground state energy solution is $E_0^{\text{HF}}(\alpha_{\text{I}})$, while for $v + w \geq 1$ the solution is $E_0^{\text{HF}}(\alpha_{\text{II}})$. On top of that, if $v + w = 1$ the solutions $E_0^{\text{HF}}(\alpha_{\text{I}})$ and $E_0^{\text{HF}}(\alpha_{\text{II}})$ are equal.

In conclusion, for the ground state energy given by the HF mean-field approximation we write

$$E_0^{\text{HF}} = \begin{cases} -\varepsilon\frac{N}{2}\left(1 + \frac{w}{N-1}\right), & v+w < 1, \\ -\varepsilon\frac{N}{4}\left[\frac{2w}{N-1} + \frac{1+(v+w)^2}{v+w}\right], & v+w \geq 1. \end{cases} \tag{2.3.22}$$

The final result in Eq. (2.3.22) agrees with that in [10, 11]. At this point, we leave the discussion concerning the HF solution to Chapter 3, where we introduce a more sophisticated beyond mean-field many-body method.

Chapter 3

Random Phase Approximation

3.1   Collective vibrations & Excitations

The goal of present Section 3.1 is to give a phenomenological overview of collective vibrations and correlations of states in many-body quantum systems. Subsequently, we want to set up a theoretical framework, that would allow one to treat beyond-mean field effects and the construction of the excited states.

In the case of the Hartree-Fock mean-field approach, studied in Chapter 2, the idea was to approximate the exact eigenvalue problem by the construction of an effective mean-field $\widetilde{V}$, thus reducing a multi-body interaction problem to a one-body interaction only. This way, we sought to find the ground state $|\Phi\rangle$. We then minimized the total mean energy given as $E[|\Phi\rangle] = \langle H\rangle$, which corresponded to $|\Phi\rangle$. To achieve this, the variational principles were employed, and the minimal HF energy E_0^{HF} provided an upper bound on the exact ground state energy E_0. One can of course seek to do better, and try to fill this upper bound gap by introducing interaction perturbations to the HF mean-field. Moreover, with further elaboration, one could also attempt to construct the excited states.

Let us examine some of the microscopic properties that are common to many-body quantum systems. Several examples mentioned in [8] are collective vibrations or mutual correlations between the many-particle states. These often provide non-negligible energy contributions to the spectra and need to be accounted for. To track these effects, one can, for instance, take the shell-model predictions and compare them with the actual experimental data and look for discrepancies. In the case of low-lying
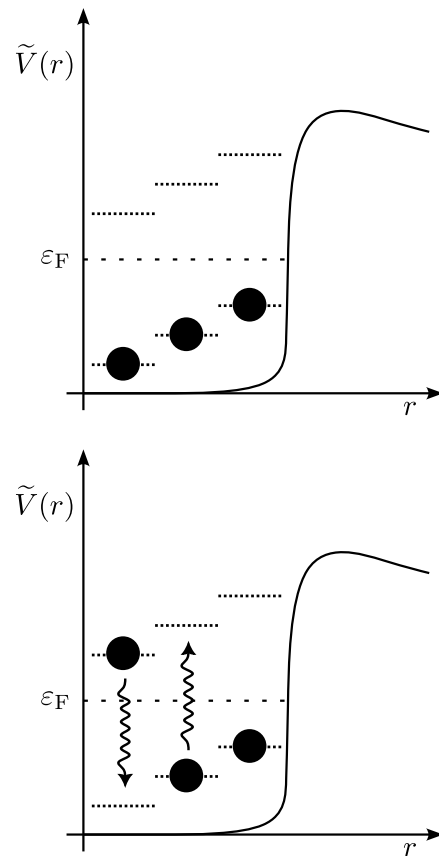
Figure 3.1.1   Schematic showing the idea of HF mean-field and 1p-1h excitations.

excited states, these missing energy effects are often due to collective vibrations or correlations between the states. Phenomena causing similar energy differences exist for higher-excited states as well [8]. This way, we justify a need for the so-called beyond mean-field methods, whose aim is to tackle further non-trivial contributions.

The most simple way to introduce a perturbation to a mean-field is to assume the existence of a new ground state $|0\rangle$ which in some sense captures the essence of a more detailed microscopic interaction

$$|0\rangle = X_0^0|\text{HF}\rangle + \sum_{k,l} X_{kl}^0\, a_k^\dagger a_l|\text{HF}\rangle + \frac{1}{4} \sum_{k,l,m,n} X_{klmn}^0\, a_k^\dagger a_l^\dagger a_m a_n|\text{HF}\rangle + \dots \quad (3.1.1)$$

Similar expansion to that in Eq. (3.1.1) can be, in principle, written for an arbitrary excited state $|n\rangle$

$$|n\rangle = X_0^n|\text{HF}\rangle + \sum_{k,l} X_{kl}^n\, a_k^\dagger a_l|\text{HF}\rangle + \frac{1}{4} \sum_{k,l,m,n} X_{klmn}^n\, a_k^\dagger a_l^\dagger a_m a_n|\text{HF}\rangle + \dots \quad (3.1.2)$$

Additional terms to the zero-order HF term in Eq. (3.1.1) and Eq. (3.1.2) are usually called 1p-1h excitations for the first-order term, and 2p-2h excitations for the second-order term and so on. Expansion in Eq. (3.1.1) and Eq. (3.1.2) provide a systematic way to introduce higher-order contributions to the established mean-field approximation. With these higher-order terms, it then may be possible to construct the excited states or give an explanation for some of the more complex physical phenomena.

3.2 Random Phase & Tamm-Dancoff Approximation

Two commonly used many-body methods that allow the construction of excited states stemming from the 1p-1h excitations are the Tamm-Dancoff approximation (TDA) and the random phase approximation (RPA). We start with the latter and show the TDA to be a special case of the RPA method. The latter is in fact more general and also provides a ground state correction [8].

We start by introducing excitation operator $Q^\dagger$ in the following way

$$Q^\dagger|0\rangle = |1\rangle, \quad (3.2.1)$$
$$Q\,|1\rangle = |0\rangle, \quad (3.2.2)$$
$$Q\,|0\rangle = 0, \quad (3.2.3)$$

where it is convenient to abbreviate $|0\rangle \equiv |\text{RPA}\rangle$, the new ground state which is a correction to the non-correlated mean-field ground state $|\text{HF}\rangle$ in the spirit of Eq. (3.1.1), and $|1\rangle$ denotes the first excited state.

The definition of excitation operator $Q^\dagger$ in terms of creation and annihilation operator reads [8]

$$Q^\dagger = \sum_{k,l} \left(X_{kl} a_k^\dagger a_l - Y_{kl} a_l^\dagger a_k \right), \quad (3.2.4)$$

with X_{kl} and Y_{kl} being some arbitrary coefficient giving a proper weight of the 1p-1h excitations. Quantities $|X_{kl}|^2$ and $|Y_{kl}|^2$ then provide probability amplitudes of the 1p-1h excitations.

Next, we inspect the commutator of H and $Q^\dagger$, which all in all turns out to yield the excitation energy ε when going from the ground state $|\text{RPA}\rangle$ to the first excited state $|1\rangle$

$$
\begin{aligned}
\left[H, Q^\dagger\right] |\text{RPA}\rangle = \left(HQ^\dagger - Q^\dagger H\right) |\text{RPA}\rangle = \\
= (E_1^{\text{RPA}} - E_0^{\text{RPA}})Q^\dagger|\text{RPA}\rangle = \varepsilon Q^\dagger|\text{RPA}\rangle,
\end{aligned}
\tag{3.2.5}
$$

where E_0^{RPA} is the RPA ground state energy and E_1^{RPA} gives the first excited state energy.

One can also take a variation of the excitation operator $\delta(Q^\dagger)$. Making use of this variation $\delta(Q^\dagger)$ together with Eq. (3.2.5), as discussed in [8], this way one gets all possible 1p-1h states present in the Hilbert space $\mathcal{H}$ of the given problem. This directly leads to the following set of equations

$$
\langle\text{RPA}| \left[a_k^\dagger a_l, \left[H, Q^\dagger\right]\right] |\text{RPA}\rangle = \varepsilon\langle\text{RPA}| \left[a_k^\dagger a_l, Q^\dagger\right] |\text{RPA}\rangle,
\tag{3.2.6}
$$

$$
\langle\text{RPA}| \left[a_l^\dagger a_k, \left[H, Q^\dagger\right]\right] |\text{RPA}\rangle = \varepsilon\langle\text{RPA}| \left[a_l^\dagger a_k, Q^\dagger\right] |\text{RPA}\rangle,
\tag{3.2.7}
$$

which can be verified through a direct evaluation of the commutators. Eq. (3.2.6) together with Eq. (3.2.7) define an eigenvalue problem whose solution gives an approximation to the excitation energy ε. However, no specific information regarding the new ground state $|\text{RPA}\rangle$ aside from its definition in Eq. (3.2.1) is available. To make things even worse, we have no knowledge of X_{kl} and Y_{kl} coefficients either. Nonetheless, there exists a way to solve Eq. (3.2.6) and Eq. (3.2.7).

We first seek to evaluate X_{kl} and Y_{kl} coefficients. This can be done in the following tricky way. We realize that fermionic creation and annihilation operator pairs $a_k^\dagger a_l$ can be replaced by bosonic creation and annihilation operators. Just as in [8], let us assume it is possible to evaluate the mean value of a fermionic state $|\text{RPA}\rangle$ using bosonic operators. In addition to that, let the matrix elements of $\left[a_k^\dagger a_l, a_m^\dagger a_n\right]$ appropriate to the new ground state $|\text{RPA}\rangle$ not differ too much from that of $|\text{HF}\rangle$.

Under these circumstances, we write the following [8]

$$
\langle\text{RPA}| \left[a_k^\dagger a_l, a_m^\dagger a_n\right] |\text{RPA}\rangle \approx \langle\text{HF}| \left[a_k^\dagger a_l, a_m^\dagger a_n\right] |\text{HF}\rangle \approx \delta_{kn}\delta_{lm}.
\tag{3.2.8}
$$

The approximation made in Eq. (3.2.8) is called a quasi-boson approximation (QBA). This, of course, defies the Pauli exclusion principle, in turn, however, it makes it possible to evaluate Eq. (3.2.8) and thus allowing one to find X_{kl} and Y_{kl} coefficients.

As such, the approximation in Eq. (3.2.8) turns out to be acceptable if it holds that $|X_{kl}| \gg |Y_{kl}|$[1]. If this is true, the weight of backward 1p-1h excitations is small, and violation of the Pauli exclusion principle is usually acceptable.

---

[1]This is obviously due to $|X_{kl}|^2$ and $|Y_{kl}|^2$ coefficients having the meaning of occupation probability amplitudes [8].

Armed with Eq. (3.2.8) we obtain X_{kl} and Y_{kl} coefficients simply as

$$X_{kl} = \langle \text{HF}| \left[a_l^\dagger a_k, Q^\dagger \right] |\text{HF}\rangle, \tag{3.2.9}$$

$$Y_{kl} = \langle \text{HF}| \left[a_k^\dagger a_l, Q^\dagger \right] |\text{HF}\rangle. \tag{3.2.10}$$

Usually one also defines A_{klmn} and B_{klmn} coefficients

$$A_{klmn} = \langle \text{RPA}| \left[a_l^\dagger a_k, \left[H, a_m^\dagger a_n \right] \right] |\text{RPA}\rangle, \tag{3.2.11}$$

$$B_{klmn} = -\langle \text{RPA}| \left[a_l^\dagger a_k, \left[H, a_n^\dagger a_m \right] \right] |\text{RPA}\rangle. \tag{3.2.12}$$

Assuming QBA to be valid, we can also apply it to Eq. (3.2.11) and Eq. (3.2.12). In return, Eq. (3.2.9) and Eq. (3.2.10) can be recast into the following very compact matrix equation

$$\begin{pmatrix} A & B \\ B^* & A^* \end{pmatrix} \begin{pmatrix} X \\ Y \end{pmatrix} = \varepsilon \begin{pmatrix} 1 & 0 \\ 0 & -1 \end{pmatrix} \begin{pmatrix} X \\ Y \end{pmatrix}. \tag{3.2.13}$$

In literature [8, 17, 22] the previous matrix Eq. (3.2.13) is commonly referred to as RPA equations.

Solving Eq. (3.2.13) yields the coefficients X_{kl} and Y_{kl} and excitation energy ε. This way, one can evaluate new the ground state energy E_0^{RPA} and the first excited state energy E_1^{RPA} simply as

$$E_0^{\text{RPA}} = \langle \text{RPA}|H|\text{RPA}\rangle, \tag{3.2.14}$$
$$E_1^{\text{RPA}} = \langle \text{RPA}|QHQ^\dagger|\text{RPA}\rangle. \tag{3.2.15}$$

More details concerning the RPA equations, their solutions, or numerical implementation are given in [8].

At last, we return to the TDA method briefly mentioned at the beginning of Section 3.2. In some sense, the idea behind the TDA is similar to that of the RPA method. The main difference is that the TDA method is built on the HF mean-field $|\text{HF}\rangle$ ground state, and thus limits itself to the excited states only. One assumes excitation operator $Q^\dagger$ to bring the system from the ground state to the first excited state

$$Q^\dagger|\text{HF}\rangle = |1\rangle, \tag{3.2.16}$$

with $|1\rangle$ denoting the first excited state.

In the TDA method, a general form of $Q^\dagger$ is assumed to be

$$Q^\dagger = \sum_{k,l} X_{kl} a_k^\dagger a_l. \tag{3.2.17}$$

Following that, one sets out to derive TDA equations as done in [8]. The procedure is similar to that we showed for RPA equations. In the end, one obtains the following set of equations

$$\sum_{kl} X_{kl} \langle \text{HF}| \left[a_k^\dagger a_l, \left[H, a_i^\dagger a_j \right] \right] |\text{HF}\rangle = \varepsilon X_{ij}. \tag{3.2.18}$$

Notice that setting $Y_{kl} = 0$ in Eq. (3.2.13) reduces to TDA equations in Eq. (3.2.18). Overall, the TDA method is a special case of the RPA method. The main difference between the two methods is the ground state treatment and the addition of correlations to the ground state which comes with the RPA method.

3.3 RPA solution of the Lipkin model

In present Section 3.3 we apply the RPA method to the Lipkin model. Once we are done with the RPA method, we briefly discuss the TDA solution. Then we inspect the properties of the RPA solution and we give a comparison for both the RPA and the HF solutions, which were discussed in Section 2.2, to the exact solutions of the model.

First, we note the whole of the RPA approach is formulated in the HF mean-field basis. In particular, we operate in mean-field basis $|\widetilde{k}, \widetilde{m}\rangle$. Just as in [10], we realize internal symmetry and set $X_{kl} \equiv X$ together with $Y_{kl} \equiv Y$ $\forall k, l$, and therefore we define excitation operator $Q^\dagger$ as

$$Q^\dagger = \frac{1}{\sqrt{N}} \sum_{k,l}^{\Omega} \left(X_{kl}\, \widetilde{a}_{k+}^\dagger\, \widetilde{a}_{l-} - Y_{kl}\, \widetilde{a}_{l-}^\dagger\, \widetilde{a}_{k+} \right) = \frac{X\widetilde{K}_+ - Y\widetilde{K}_-}{\sqrt{N}}, \qquad (3.3.1)$$

with $\widetilde{K}_\pm$ being same operators in the HF mean-field $|\widetilde{k}, \widetilde{m}\rangle$ basis as in Eq. (2.3.12) and $X, Y \in \mathbb{C}$. A phase for both X and Y can be chosen in such a way that both quantities end up becoming real numbers.

Assuming $|\text{RPA}\rangle$ to be the new ground state, and $|1\rangle$ being the first excited state, for $Q^\dagger$ we demand

$$Q^\dagger|\text{RPA}\rangle = |1\rangle, \qquad (3.3.2)$$

$$Q\,|1\rangle = |\text{RPA}\rangle, \qquad (3.3.3)$$

$$Q\,|\text{RPA}\rangle = 0. \qquad (3.3.4)$$

Following that, we rewrite Eq. (3.2.6) and Eq. (3.2.7) as

$$\langle\text{RPA}| \left[\widetilde{K}_-, \left[\widetilde{H}, Q^\dagger\right]\right] |\text{RPA}\rangle = \omega\langle\text{RPA}| \left[\widetilde{K}_-, Q^\dagger\right] |\text{RPA}\rangle, \qquad (3.3.5)$$

$$\langle\text{RPA}| \left[\widetilde{K}_+, \left[\widetilde{H}, Q^\dagger\right]\right] |\text{RPA}\rangle = \omega\langle\text{RPA}| \left[\widetilde{K}_-, Q^\dagger\right] |\text{RPA}\rangle, \qquad (3.3.6)$$

where $\widetilde{H}$ is the HF mean-field Hamiltonian from Eq. (2.3.10) and ω denotes excitation energy.

Let us define A and B coefficients as

$$A = \frac{1}{N}\langle\text{HF}| \left[\widetilde{K}_-, \left[\widetilde{H}, \widetilde{K}_+\right]\right] |\text{HF}\rangle, \qquad (3.3.7)$$

$$B = -\frac{1}{N}\langle\text{HF}| \left[\widetilde{K}_-, \left[\widetilde{H}, \widetilde{K}_-\right]\right] |\text{HF}\rangle. \qquad (3.3.8)$$

Let the matrix elements corresponding to $|\text{RPA}\rangle$ only slightly differ from those appropriate to $|\text{HF}\rangle$, and if we assume QBA to be valid, we write RPA equations for the Lipkin model

$$\begin{pmatrix} A + \omega & B \\ B^* & A - \omega \end{pmatrix} \begin{pmatrix} X \\ Y \end{pmatrix} = 0. \qquad (3.3.9)$$

Previous Eq. (3.3.9) is a system of two equations for a total of three unknowns X, Y, and ω. Thus in order to solve Eq. (3.3.9) one more equation is needed. This

independent equation can be obtained from a normalization condition for excited state $|1\rangle$

$$\langle 1|1 \rangle = 1. \tag{3.3.10}$$

If we expand Eq. (3.3.11) and assume a QBA, and the ground state approximation for matrix elements, we get

$$1 = \langle \text{RPA}|QQ^\dagger|\text{RPA}\rangle = \langle \text{RPA}|[Q, Q^\dagger]|\text{RPA}\rangle \approx \langle \text{HF}|[Q, Q^\dagger]|\text{HF}\rangle \approx 1, \tag{3.3.11}$$

which brings us to the third required equation

$$X^2 - Y^2 = 1. \tag{3.3.12}$$

RPA equations in Eq. (3.3.9) provide the following system of equations

$$(A - \omega)X + BY = 0, \tag{3.3.13}$$
$$B^*X + (A + \omega)Y = 0. \tag{3.3.14}$$

Solving Eq. (3.3.12), Eq. (3.3.13) and Eq. (3.3.14) yields

$$\omega = \sqrt{A^2 - |B|^2}, \tag{3.3.15}$$

$$X^2 = \frac{A + \omega}{2\omega}, \tag{3.3.16}$$

$$Y^2 = \frac{A - \omega}{2\omega}, \tag{3.3.17}$$

with coefficients A and B being given by their definition in Eq. (3.3.7) and Eq. (3.3.8). We evaluate Eq. (3.3.7) and Eq. (3.3.8) in Appendix A. The resulting form of A and B is

$$A = \varepsilon \begin{cases} 1 - w, & v + w < 1, \\ \frac{3(v+w)^2 - 1}{2(v+w)} - w, & v + w \geq 1, \end{cases} \tag{3.3.18}$$

$$B = \varepsilon \begin{cases} -v, & v + w < 1, \\ w - \frac{(v+w)^2 + 1}{2(v+w)}, & v + w \geq 1. \end{cases} \tag{3.3.19}$$

Eq. (3.3.18) and Eq. (3.3.19) are in agreement with those in [10].

At last, we set out to find the ground state energy E_0^{RPA} corresponding to $|\text{RPA}\rangle$ state. To get E_0^{RPA}, we could either directly evaluate the mean ground state energy, or assume and verify it to be the sum of the HF mean-field energy E_0^{HF} and an additional contribution which is due to correction term h

$$E_0^{\text{RPA}} = \langle \text{RPA}|\widetilde{H}|\text{RPA}\rangle = E_0^{\text{HF}} + \langle \text{RPA}|h|\text{RPA}\rangle. \tag{3.3.20}$$

The correction h is given by

$$h = \frac{A}{N}\widetilde{K}_+\widetilde{K}_- + \frac{B}{2N}\left(\widetilde{K}_+^2 + \widetilde{K}_-^2\right). \tag{3.3.21}$$

To obtain the form of h from Eq. (3.3.21) one has to substitute for $\widetilde{H}$ in Eq. (3.3.20), and carry out the cumbersome calculation with $\widetilde{H}$ given in Eq. (2.3.9). No

discussion concerning the form of h in Eq. (3.3.21) is given in either [10, 11]. However, a clever way around how to derive Eq. (3.3.21) is to substitute h from Eq. (3.3.21) to both Eq. (3.3.7) and Eq. (3.3.8) and to show these to hold (for details see Appendix A).

We return to Eq. (3.3.20) and the calculation of E_0^{RPA}. To evaluate Eq. (3.3.20), namely the h term, we need to find the following matrix elements $\langle 0|\widetilde{K}_\pm \widetilde{K}_\mp|0\rangle$ and $\langle 0|\widetilde{K}_\pm^2|0\rangle$, where we denote $|0\rangle \equiv |\mathrm{RPA}\rangle$.

One way to do this is simply to exploit properties of $Q^\dagger$. From definition in Eq. (3.3.1) it follows that

$$\langle 1|\widetilde{K}_+|0\rangle = \sqrt{N}X, \qquad \langle 1|\widetilde{K}_-|0\rangle = \sqrt{N}Y. \tag{3.3.22}$$

If we add two more matrix elements $\langle 0|Q^\dagger Q|0\rangle = 0$ and $\langle 0|QQ^\dagger|0\rangle = 1$ and expand Eq. (3.3.22)^2, we end up with the following system of four equations

$$N = \langle 0|Y^2\widetilde{K}_+\widetilde{K}_- + X^2\widetilde{K}_-\widetilde{K}_+ - XY\widetilde{K}_+^2 - XY\widetilde{K}_-^2|0\rangle, \tag{3.3.23}$$

$$0 = \langle 0|X^2\widetilde{K}_+\widetilde{K}_- + Y^2\widetilde{K}_-\widetilde{K}_+ - XY\widetilde{K}_+^2 - XY\widetilde{K}_-^2|0\rangle, \tag{3.3.24}$$

$$\sqrt{N}X = \frac{1}{\sqrt{N}}\langle 0|X\widetilde{K}_-\widetilde{K}_+ - Y\widetilde{K}_+^2|0\rangle, \tag{3.3.25}$$

$$\sqrt{N}Y = \frac{1}{\sqrt{N}}\langle 0|X\widetilde{K}_-^2 - Y\widetilde{K}_+\widetilde{K}_-|0\rangle. \tag{3.3.26}$$

With the aid of Eq. (3.3.12), the preceding system from Eq. (3.3.23) to Eq. (3.3.26) can be solved for each of the matrix elements. The solution is

$$\langle 0|\widetilde{K}_+\widetilde{K}_-|0\rangle = NY^2, \qquad \langle 0|\widetilde{K}_-\widetilde{K}_+|0\rangle = NX^2,$$
$$\langle 0|\widetilde{K}_+^2|0\rangle = NXY, \qquad \langle 0|\widetilde{K}_-^2|0\rangle = NXY. \tag{3.3.27}$$

As of now, we have everything we need to evaluate ground state energy E_0^{RPA} in Eq. (3.3.20). The calculation in Eq. (3.3.20) follows as

$$E_0^{\mathrm{RPA}} = E_0^{\mathrm{HF}} + \langle 0|h|0\rangle = E_0^{\mathrm{HF}} + \frac{A}{N}\langle 0|\widetilde{K}_+\widetilde{K}_-|0\rangle + \frac{B}{2N}\langle 0|\widetilde{K}_+^2|0\rangle + \frac{B}{2N}\langle 0|\widetilde{K}_-^2|0\rangle =$$
$$= E_0^{\mathrm{HF}} + AY^2 + \frac{B}{2N}XY + \frac{B}{2N}XY = E_0^{\mathrm{HF}} - \omega Y^2, \tag{3.3.28}$$

where we have employed Eq. (3.3.12). The formula in Eq. (3.3.28) for the ground state energy E_0^{RPA} is equivalent to that provided in [10, 11].

If we further substitute back ω and Y^2 quantities from Eq. (3.3.15) and Eq. (3.3.17), by using results from Eq. (3.3.18) and Eq. (3.3.19), we obtain an explicit form of E_0^{RPA}

$$E_0^{\mathrm{RPA}} = \begin{cases} E_0^{\mathrm{HF}}(\alpha_{\mathrm{I}}) + \frac{\varepsilon}{2}\left(w - 1 + \sqrt{(1-w)^2 - v^2}\right), & v + w < 1, \\ E_0^{\mathrm{HF}}(\alpha_{\mathrm{II}}) + \varepsilon\left(\frac{1-3v^2-4vw-w^2}{4(v+w)} + \sqrt{\frac{v(v^2+2vw+w^2-1)}{2(v+w)}}\right), & v + w \geq 1, \end{cases} \tag{3.3.29}$$

---

^{2}Which also explains why Eq. (3.3.22) holds true.

with $E_0^{\text{HF}}(\alpha_{\text{I}})$ given by Eq. (2.3.18) and $E_0^{\text{HF}}(\alpha_{\text{II}})$ given in Eq. (2.3.19).

Since quantity ω is just the excitation energy, adding it to E_0^{RPA} produces the first excited state energy. Moreover, since we are dealing with QBA [8], the RPA method is in fact a harmonic approximation, with the spectrum having the same structure as that of a linear harmonic oscillator. Simply put, the energy of an arbitrary excited state $|n\rangle$ is just
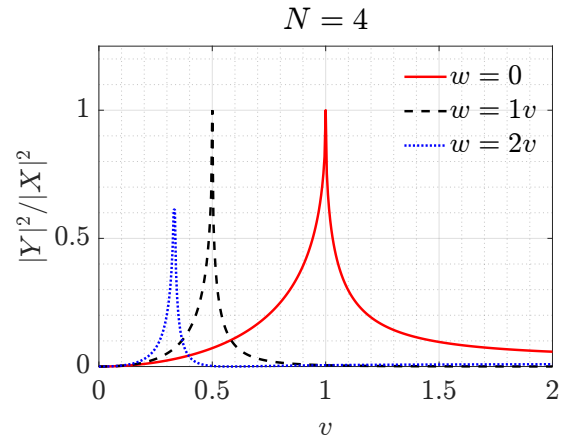
$$E_n^{\text{RPA}} = E_0^{\text{HF}} + \omega(n - Y^2) = E_0^{\text{RPA}} + \omega n. \tag{3.3.30}$$

Now, the very same could be done for the TDA method, however, in Section 3.2 we showed it to be a special case of the RPA. Setting $Y = 0$ in Eq. (3.3.30) and taking only the first excited state, we get the TDA approximation for the energy of the first excited state $|1\rangle$.
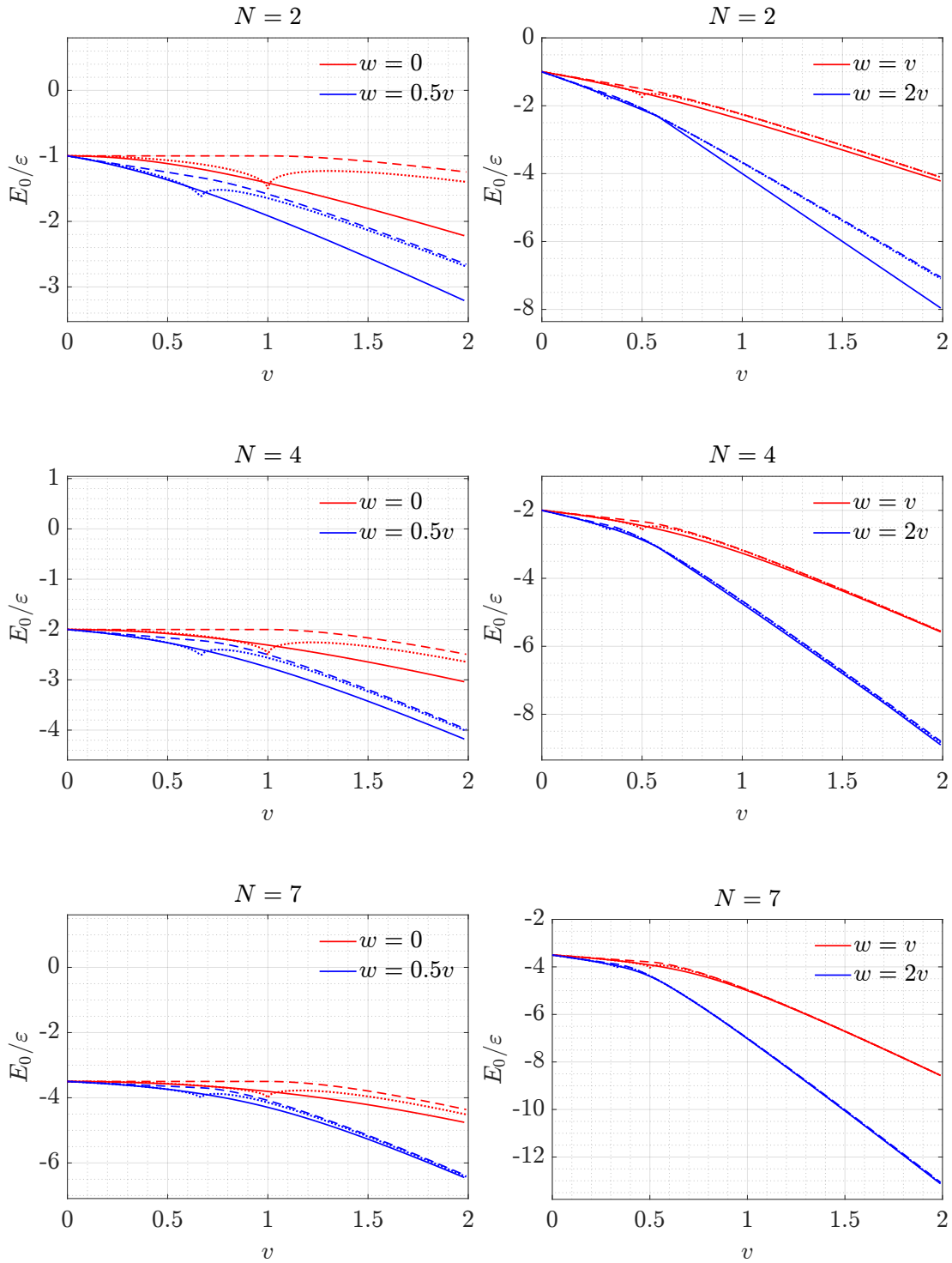
Next, we turn our attention to the features of the RPA solution of the Lipkin model. Namely, we focus on the approximation performance, and its validity with respect to the QBA, and we examine what exactly happens at the point, where the exact solutions exhibit a phase transition in the case of a pure interaction W.

To begin with, we verify the QBA. In Fig. 3.3.1 we plot Y^2/X^2 quotient as a function of v for a few values of w and fixed value of particle number $N = 4$. Near points where $v+w = 1$, we see the QBA breaks, with $Y^2/X^2 \to 1$. Thus, the RPA solution has to be taken with care near these points. Otherwise, we see that the QBA is valid and the RPA solution should provide a decent approximation for energies. Also, note that the QBA becomes even better once interaction W is turned on and brought up.

Figure 3.3.1 Plot of occupation amplitudes Y^2/X^2 quotient as a function of v for fixed particle number $N = 4$ and given interaction strength w.

To compare approximation quality for all the methods considered so far (RPA, TDA, and HF), in Fig. 3.3.2 to Fig. 3.3.5 we plot the solutions for exact energy and energies obtained by various many-body methods as functions of either v or w parameters for given values of particle number N. In Fig. 3.3.2 and Fig. 3.3.3 we compare the ground state energy and show the exact solution (solid lines), the HF solution (dashed lines), and the RPA solution (dotted lines). In Fig. 3.3.4 we compare the first excited state energy, and in Fig. 3.3.5 we compare the second excited state energy of the exact solution (solid line) to the RPA solution (dotted lines), and for the first excited state we also plot the TDA solution (circle markers). We remark that the second excited state energy estimate is obtained from the harmonic extension of the RPA solutions in Eq. (3.3.30).

Figure 3.3.2 Relative ground state energy E_0/ε plot as a function of interaction strength v, for given values of interaction strength w and for given particle number N. We compare the exact solution (solid lines) with the HF method (dashed lines) and RPA method solutions (dotted lines).
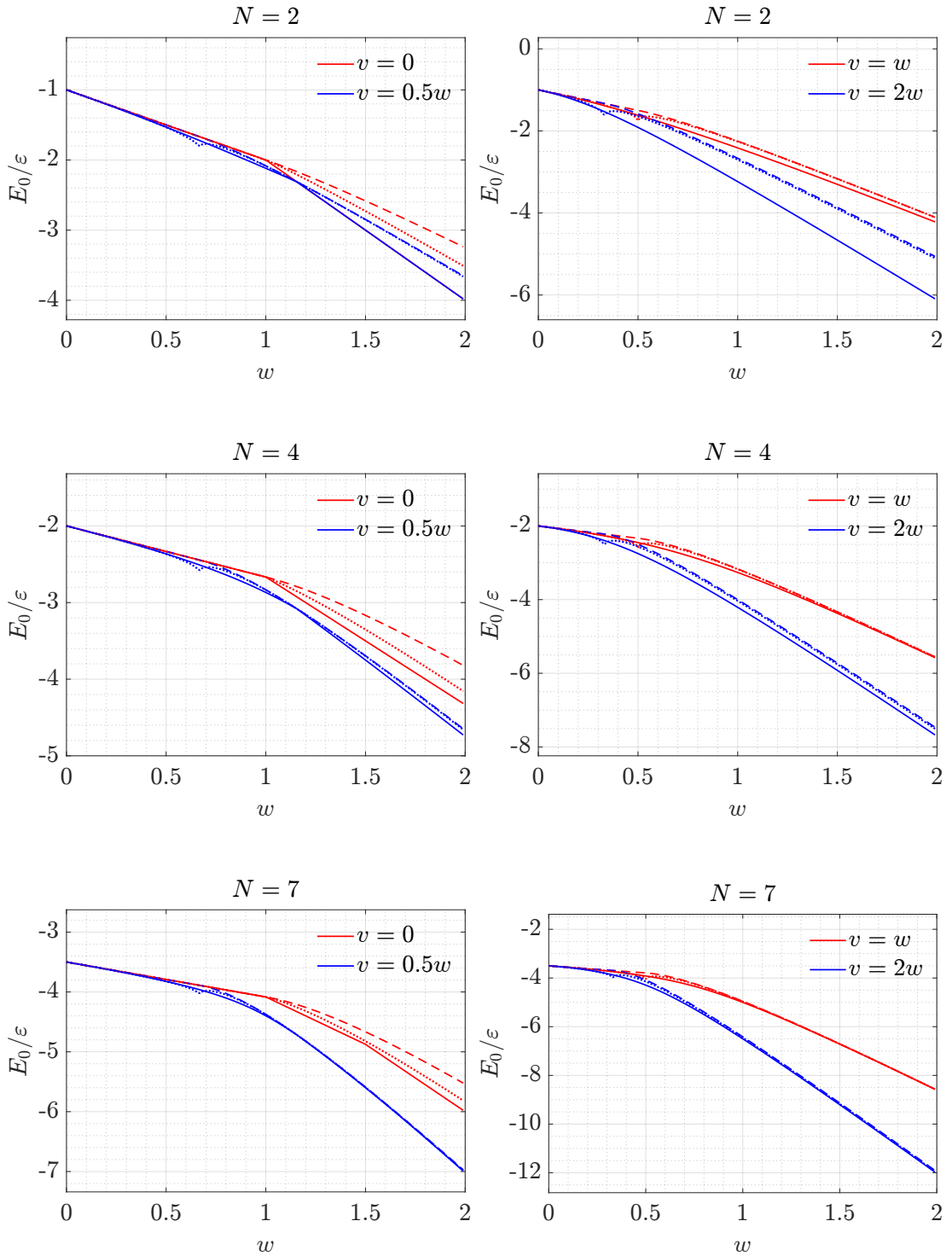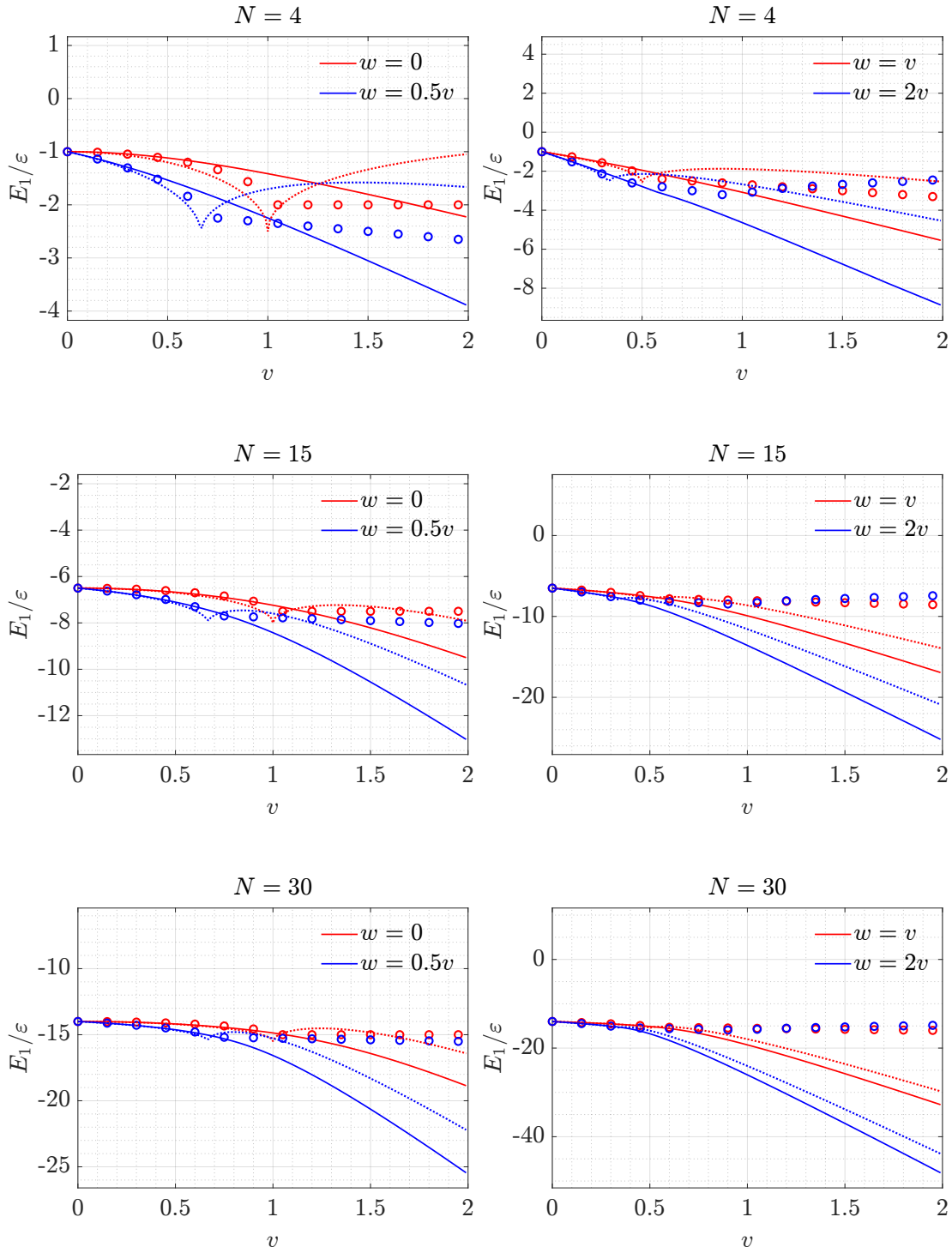
Figure 3.3.3 Relative ground state energy E_0/ε plot as a function of interaction strength w, for given values of interaction strength v and for given particle number N. We compare the exact solution (solid lines) with the HF method (dashed lines) and RPA method solutions (dotted lines).

Figure 3.3.4 The first excited state relative energy E_1/ε plot as function of interaction strength v, for given interaction strength w and for given particle number N. We compare the exact solution (solid lines) with the RPA method (dotted lines) and TDA method solutions (circle markers).

Figure 3.3.5 The second excited state relative energy E_2/ε plot as function of interaction strength v, for given interaction strength w and for given particle number N. We compare the exact solutio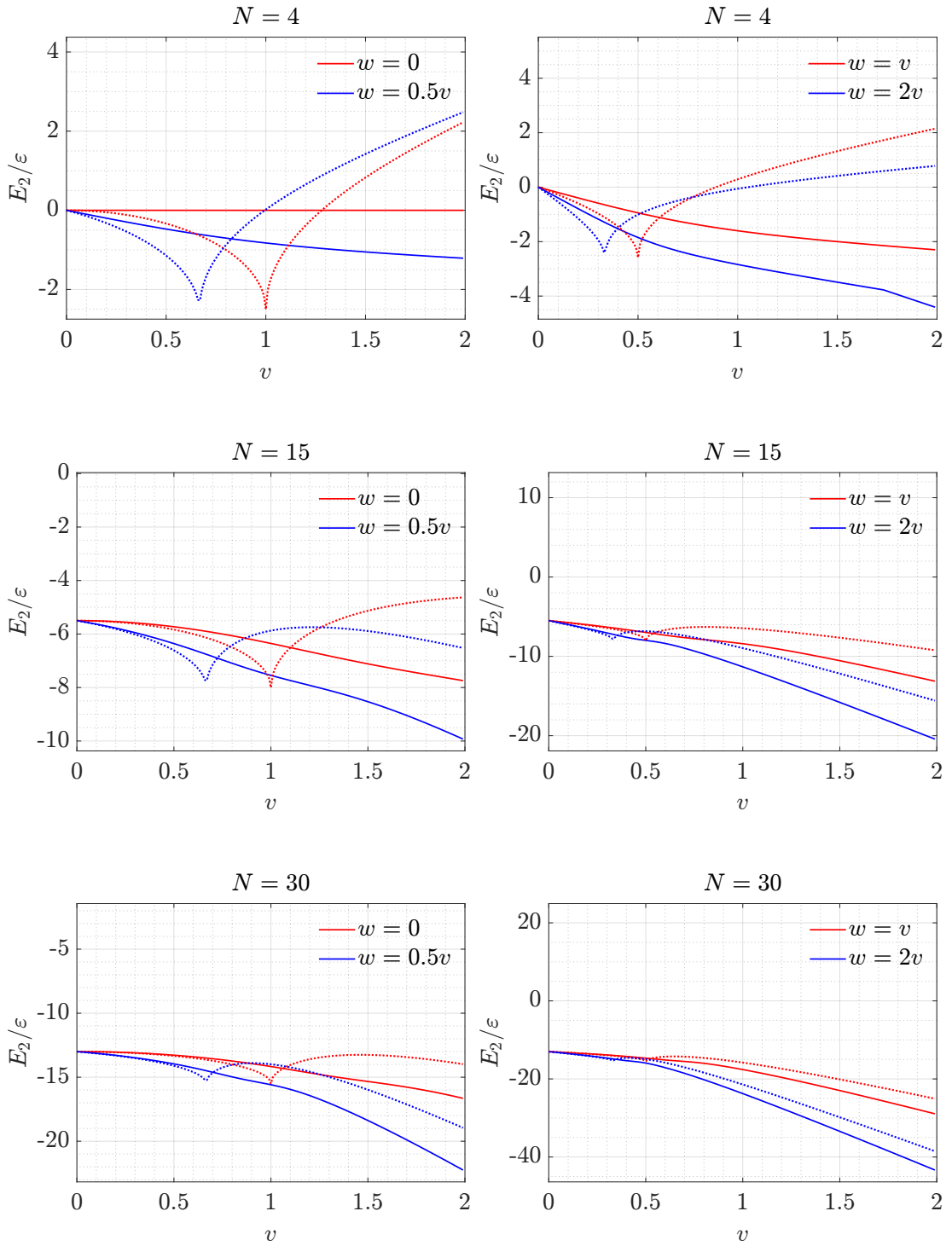n (solid lines) with the RPA method solution (dotted lines). Where the second excited state energy is obtained in the harmonic approximation from in Eq. (3.3.30).

In Fig. 3.3.2 to Fig. 3.3.5 we observe that both the RPA and the TDA methods provide a decent approximation for the ground state and excited states energies up until the point where $v + w = 1$. As for the ground state energy only, essentially the RPA method always provides a better approximation, which is especially significant for a few-particle system with N being low. When $v = 0$ and $w \leq 1$, we see that both the HF and the RPA method produce the exact solution ground state energy. This is very likely due to H being a diagonal matrix. The likely reason why this breaks up for $w \geq 1$ is the PT which occurs at $w = 1$ point. A more detailed discussion of this particular problem is postponed to the end of present Section 3.3. Also notice that as N increases, the spike at $v + w = 1$, where the QBA is strictly violated is smoothed out. This point is sometimes referred to as an RPA collapse point [10].

Although the RPA solution is continuous at the collapse point, its derivatives do not exist. To show this, we take energy E_0^{RPA} in Eq. (3.3.29), and we differentiate it with respect to either v or w. This, in general leads to the following

$$\frac{\mathrm{d}E_0^{\mathrm{RPA}}}{\mathrm{d}v}, \ \frac{\mathrm{d}E_0^{\mathrm{RPA}}}{\mathrm{d}w} \sim \sqrt{\frac{1}{v + w - 1}}. \tag{3.3.31}$$

Derivatives in Eq. (3.3.31) are eventually not defined at $v + w = 1$ point. Despite that, the RPA solution is better at the collapse point than the corresponding HF solution.

In some sense, we can think of this collapse as some sort of a PT which takes place in the RPA solution. Consequently, when $v = 0$, this makes sense with respect to the exact solution, because as we saw in Section 1.2, there is always a PT in the ground state energy E_0 at $w = 1$ point. Thus for a system with a pure interaction W, the collapse point only reflects the existence of the PT in the ground state energy, which in turn is the physical explanation for the collapse point.
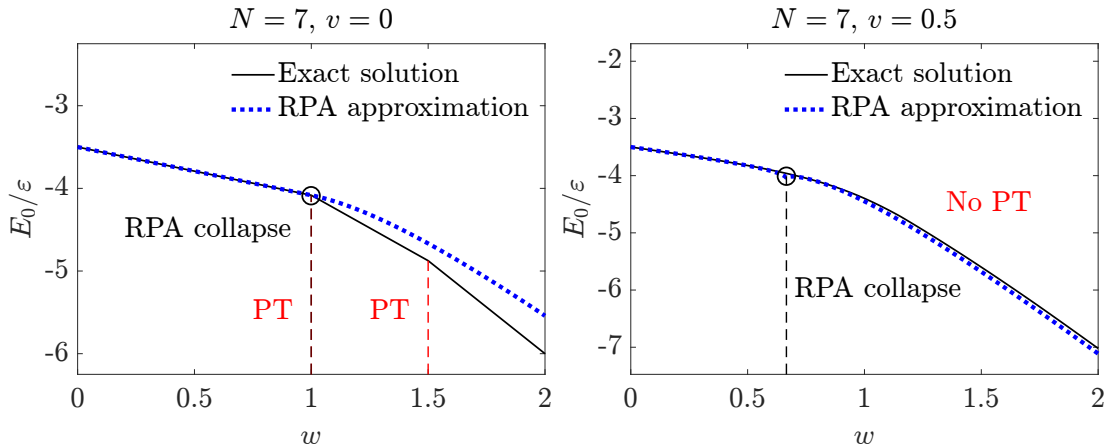
Figure 3.3.6 Relative ground state energy E_0/ε plot displaying the exact solution (solid black line) and the corresponding RPA solution (blue dotted line) as a function of w for fixed particle number $N = 7$ and for given v. Red dashed lines highlight phase transition points (PTs), and the black dashed line, together with the black circle, marks the RPA collapse point. For comparison, the plot Fig. 1.1.1 shows the whole spectra for these plotted systems.

However, this explanation does not work once interaction V is introduced. As we demonstrate in Fig. 3.3.6, when $v > 0$, the PT point at $w + v = 1$, which happens if $v = 0$, disappears due to interaction V. What is more, it is the interaction V that causes the PT points to disappear. It is also true that no more collapse points appear for higher values of w, despite more PTs taking place in the exact spectra as shown in Fig. 1.1.1. Overall, it seems the RPA method tends to treat the two interactions V and W in a similar and somewhat rather effective way, causing special features of both interactions to mix or disappear. On the other hand, as we saw in Chapter 1 if one includes both interactions V and W, the two are going to couple which then produces some extra effects to appear. Hence, it may be that coupling that comes with the RPA method might be inadequate.

Either way, a rather general physical explanation may be due to the QBA failure, which in other words, means that the Pauli exclusion principle is strongly violated at the point of collapse. This explanation may be unsatisfying to some degree, as it does not provide a precise microscopic explanation of what happens at the point of collapse.

The other way around is to closely inspect the HF mean-field solution. In Section 2.3, we found two different solutions of E_0^{HF}, each being valid for different values of v and w, with $v + w = 1$ being the transition point between them.

From a mathematical point of view, it is no coincidence that $v + w = 1$ is both the transition point for E_0^{HF} solution and the collapse point for E_0^{RPA} solution. From Section 2.3, we know that E_0^{HF} is a continuous function at the transition point, the same is true for its first derivatives.

This can be easily checked from Eq. (2.3.22)

$$\frac{\mathrm{d} E_0^{\mathrm{HF}}}{\mathrm{d} v} = \frac{\mathrm{d} E_0^{\mathrm{HF}}}{\mathrm{d} w} = -\frac{\varepsilon N}{N - 1}, \qquad \text{when} \quad v + w = 1, \qquad (3.3.32)$$

which is true for both left and right limits $(v + w) \to 1^{\pm}$.

If we differentiate E_0^{HF} one more time, we get

$$\frac{\mathrm{d}^2 E_0^{\mathrm{HF}}}{\mathrm{d} v^2} = \frac{\mathrm{d}^2 E_0^{\mathrm{HF}}}{\mathrm{d} w^2} = \begin{cases} 0, & v + w \to 1^-, \\ -\frac{\varepsilon N}{2}, & v + w \to 1^+. \end{cases} \qquad (3.3.33)$$

The second derivatives in Eq. (3.3.33) are not continuous at the transition point $v + w = 1$. In other words, there is also a PT[3] that occurs at the transition point, but this time in the HF mean-field solution.

As such, that gives us a heuristic explanation for the collapse point. To see this, we need to realize the following. If there is a second-order discontinuity in E_0^{HF} one can therefore expect a first-order discontinuity to appear once a higher order term is added to E_0^{HF} approximation. Recalling the overview in Section 3.1, we have already discussed that the core idea that underlies the RPA method, or any other similar many-body method is to include higher-order perturbation terms on top of an already established mean-field approximation. In conclusion, the foremost reason for the RPA collapse may eventually be due to the established mean-field approximation.

---

[3]Considering the second derivatives of the potential to be ill-defined, we could call it this to be a second-order phase transition.

3.4 RPA - Iterative Extension method

Based on a note made in [8] when discussing properties of RPA equations, in present Section 3.4, we build upon an idea of an iterative extension of the RPA method. First, we go through the main idea of this approach as stated in [8] and then adjust this method for numerical purposes. Namely, we reduce RPA equations in Eq. (3.2.13) to a symmetric eigenvalue problem. We then apply the proposed method to the Lipkin model from Section 1.1, and we compare its approximation quality to all the methods considered in the thesis so far. Since this method is an iterative extension of the standard RPA method, we call it the random phase approximation - iterative extension method (RPAIE).

To start, we choose a system and some arbitrary values of parameters describing the system for which we want to solve the RPA equations. From Eq. (3.2.11) and Eq. (3.2.12), we find the initial values of A and B. Having those, we can evaluate X_{kl} in Eq. (3.2.9) and Y_{kl} in Eq. (3.2.10). The RPA ground state $|\text{RPA}\rangle$ is then given by

$$|\text{RPA}\rangle = \exp\left\{ \frac{1}{2} \sum_{k,l,m,n} Y_{mn} \left(X_{kl}^*\right)^{-1} a_m^\dagger a_n a_k^\dagger a_l \right\} |\text{HF}\rangle, \qquad (3.4.1)$$

which follows from Thouless' theorem [8] when applied to $Q^\dagger$ excitation operator of form in Eq. (3.2.4), for details see [8]. Having found the ground state $|\text{RPA}\rangle$, one can return to the original RPA equations in Eq. (3.2.13) and solve them again. This time however, it is possible to directly evaluate both A and B coefficients in Eq. (3.2.11) and in Eq. (3.2.12). Then, we find new values of X, Y, and ω in Eq. (3.2.13).

To make things simple, Eq. (3.2.13) can be rewritten in the following symmetric form [8], which reduces the original generalized eigenvalue problem in Eq. (3.2.13) to an ordinary eigenvalue problem

$$S^{1/2} \begin{pmatrix} 1 & 0 \\ 0 & -1 \end{pmatrix} S^{1/2} \begin{pmatrix} \widetilde{X} \\ \widetilde{Y} \end{pmatrix} = \omega \begin{pmatrix} \widetilde{X} \\ \widetilde{Y} \end{pmatrix}, \qquad (3.4.2)$$

with S transformation matrix given as

$$S = \begin{pmatrix} A & B \\ B^* & A^* \end{pmatrix}, \qquad (3.4.3)$$

and eigenvector $(\widetilde{X}, \widetilde{Y})^{\text{T}}$ expressed in terms of $(X, Y)^{\text{T}}$ is

$$\begin{pmatrix} X \\ Y \end{pmatrix} = S^{-1/2} \begin{pmatrix} \widetilde{X} \\ \widetilde{Y} \end{pmatrix}. \qquad (3.4.4)$$

Symmetric eigenvalue problem in Eq. (3.4.2) can be solved by numerical means. This procedure can be then iterated. Having found new values of A, B, X, and Y, one can return back to Eq. (3.4.1) and find even better ground state approximation $|\text{RPA}\rangle$ and so on. Since this procedure avoids QBA in its post-initial iterations, it should in theory provide a better approximation than the standard RPA method.

We now apply this method to the Lipkin model introduced in Section 1.1. Since the solution has to be found numerically, we summarize the numerical procedure in the following scheme.

(1.) From Eq. (3.3.16) a Eq. (3.3.17) we compute starting values of X and Y.

(2.) Substituting X and Y back to Eq. (3.4.1) we find the new ground state given as

$$|\text{RPA}\rangle = \exp\left\{\frac{Y}{2NX^*}K_+^2\right\}|\text{HF}\rangle.$$

(3.) Next we refine A and B

$$A = \frac{1}{N}\langle\text{RPA}|\left[\widetilde{K}_-,\left[\widetilde{H},\widetilde{K}_+\right]\right]|\text{RPA}\rangle,$$
$$B = -\frac{1}{N}\langle\text{RPA}|\left[\widetilde{K}_-,\left[\widetilde{H},\widetilde{K}_-\right]\right]|\text{RPA}\rangle.$$

(4.) We solve symmetric eigenvalue problem in Eq. (3.4.2)

$$S^{1/2}\begin{pmatrix}1 & 0 \\ 0 & -1\end{pmatrix}S^{1/2}\begin{pmatrix}\widetilde{X} \\ \widetilde{Y}\end{pmatrix} = \varepsilon\begin{pmatrix}\widetilde{X} \\ \widetilde{Y}\end{pmatrix},$$

and obtain new values of ω, X and Y.

(5.) With $\widetilde{H}$ from Eq. (2.3.10) we evaluate E_0^{RPA}

$$E_0^{\text{RPA}} = \langle\text{RPA}|\widetilde{H}|\text{RPA}\rangle.$$

(6.) If the new E_0^{RPA} approximation is good enough, we stop, otherwise we return to (2.), and the cycle is repeated with last values of X and Y.

In Fig. 3.4.1 and Fig. 3.4.2, the left panels show a plot of relative ground state energy as a function of v for given values of w and N. We plot E_0/ε for the exact solution (solid black lines), the RPA solution from Section 3.3 and for the RPAIE solution with a number of iterations $i = 1$ (red dashed line), and $i = 5$ (blue dash-dotted line). The right panels display plots of relative approximation error $|\Delta E_0|/E_0$ for all these methods. Where the relative approximation error is defined as $|\Delta E_0|/E_0 \equiv |E_0^{\text{exact}} - E_0^{\text{Approx}}|/E_0^{\text{exact}}$.
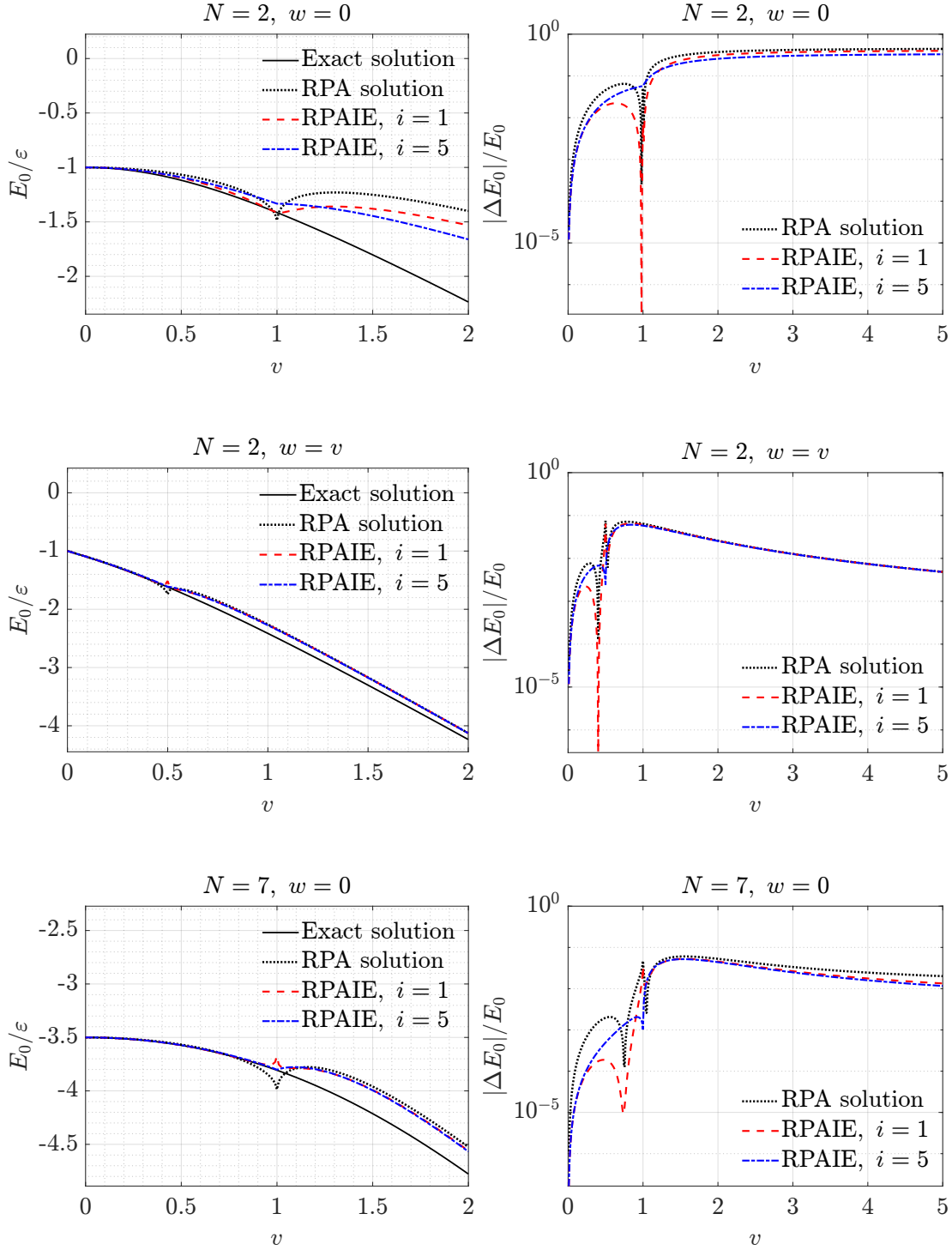
Figure 3.4.1 Left panels display a plot of the relative ground state energy E_0/ε as a function of interaction strength v for given values of N and given w. We plot the exact solution (solid black lines), the RPA solution (black dotted lines), and the RPAIE solutions with a number of iterations $i = 1$ (red dashed lines) and $i = 5$ (blue dash-dotted lines). Right panels show the corresponding relative approximation error $|\Delta E_0|/E_0$.
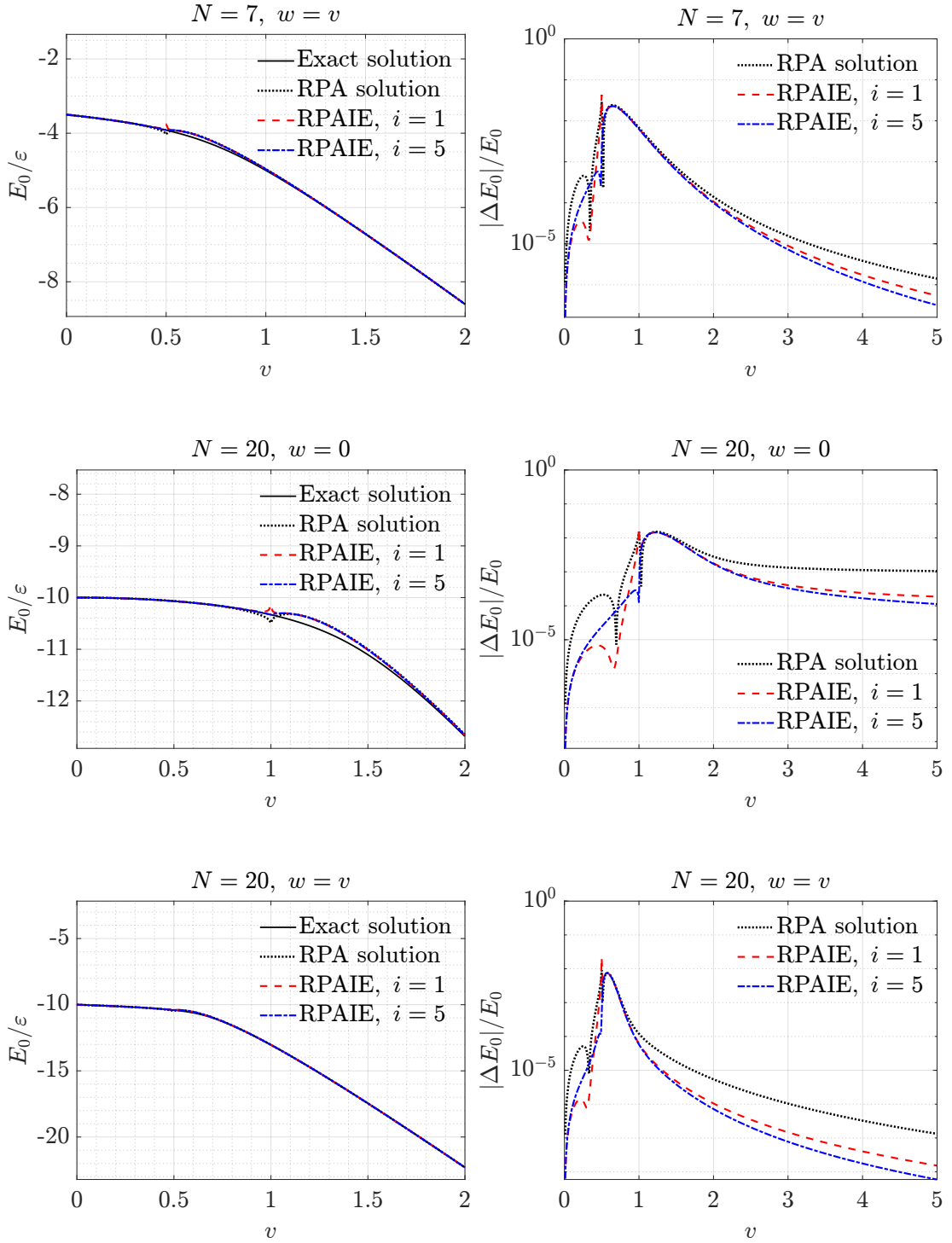
Figure 3.4.2 Left panels display a plot of the relative ground state energy E_0/ε as a function of interaction strength v for given values of N and given w. We plot the exact solution (solid black lines), the RPA solution (black dotted lines), and the RPAIE solutions with a number of iterations $i = 1$ (red dashed lines) and $i = 5$ (blue dash-dotted lines). Right panels show the corresponding relative approximation error $|\Delta E_0|/E_0$.

From previous Fig. 3.4.1 and Fig. 3.4.2, especially from all plots depicting relative approximation error $|\Delta E_0|/E_0$, we see the RPAIE method with a number of iterations $i = 5$ to be superior to the standard RPA method, for both small and large values of interaction strength v. Usually, at the point of RPA collapse, it happens that the standard RPA gives a similar approximation to ground state energy E_0, however, as discussed in Section 3.3, this appears to happen by chance, as there is no objective justification for the RPA method to give a meaningful approximation near the collapse point at all.

Aside from that, we also notice the RPAIE with a number of iterations $i = 1$ provides a better result than the standard RPA but not as good as the RPAIE with a higher number of iterations. More iterations may be used to get an even better approximation, however, a number of iterations $i = 5$ provides a result good enough.

In Fig. 3.4.1 and Fig. 3.4.2, we observe the RPAIE approximation improves as particle number N increases. To verify this, in Fig. 3.4.3, we give a relative error $|\Delta E_0|/E_0$ comparison for the HF, the RPA, and the RPAIE methods for fixed values of v and w as a function of N, with $\Delta N = 3$ step, and the initial value of N given as $N_0 = 2$.
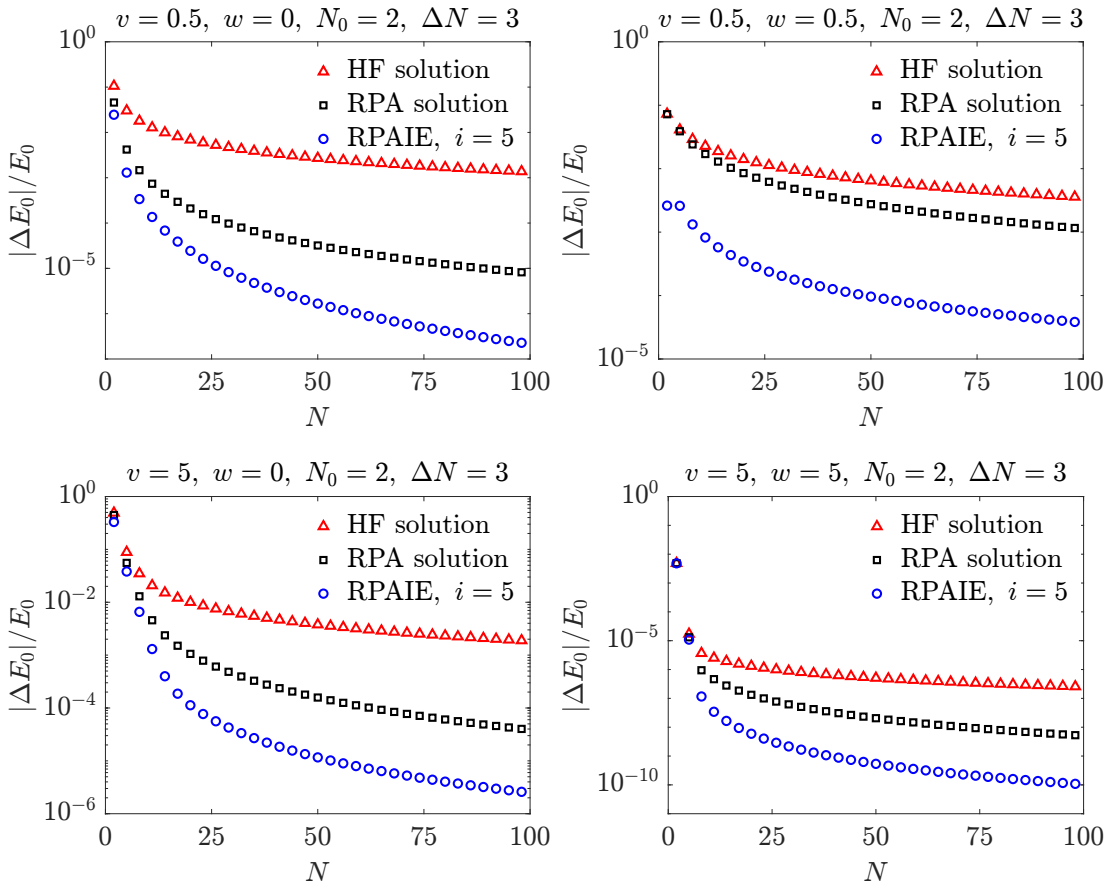
Figure 3.4.3 Plot of $|\Delta E_0|/E_0$ relative energy error as a function of particle number N, with $\Delta N = 3$ step in N and initial value of particle number $N_0 = 2$ for given values of interaction strengths v a w. We give a comparison to the HF solution (red triangles), the standard RPA solution (black boxes), and the RPAIE with $i = 5$ number of iterations (blue circles).

Let us now discuss some of the properties of the RPAIE method, which we can deduce from Fig. 3.4.1 to Fig. 3.4.3. First, we can see it to have largely smoothed out the RPA collapse point at $v + w = 1$. This smoothing of the collapse point is not so much surprising. As discussed in Section 3.3, the collapse point occurs due to the QBA not being valid. As we saw earlier, the RPAIE method only partly relies on the QBA when initial values of A, B, X, and Y are evaluated. Nonetheless, the collapse point does not entirely disappear, and a non-trivial change in derivatives is still present, despite nothing peculiar occurring in the exact ground state solution. Thus, it will likely be a remnant of the original RPA solution. From Fig. 3.4.3, it is also clear that the RPAIE method with a number of iterations $i = 5$ leads, by far, to the best ground state energy approximation, superior to both the RPA and the HF solutions. Furthermore, it performs even better as particle number N increases. This is true for both small and large values of interaction strengths v or w. To better emphasize this, we display the $|\Delta E_0|/E_0$ plot in Fig. 3.4.3 in a log scale.

Although the RPAIE method provides an excellent approximation to the ground state energy, unlike the HF or the standard RPA method, it does not provide any explicit formula for the ground state energy E_0. This may not be an issue at all since it is always possible to plot the numerical solution and study that type of solution. On the other hand, any explicit formula usually provides a better insight into the nature of the given problem. For instance, in the case of E_0^{HF} and E_0^{RPA} we could in principle solve for $N \to +\infty$ or w, $v \to +\infty$ limits, or we could do a closer analysis of the system's behavior near the first phase transition point, and all of that purely by analytic means.

We make one last remark here. Intentionally, we left the case of a system with interaction W only to Chapter 4, where a special treatment of the interaction W is done using the BCS method.

Chapter 4

Bardeen-Cooper-Schrieffer Method

4.1   Pairing interaction

In many-particle systems such as nuclei or solids there often exists a system-specific short-range interaction, that makes particles form sort of particle-like pairs. In the case of the solids [23], its electrons whose mutual interaction combined with a lattice interaction produces a superconducting current.

As for the nuclei, there exists a nucleon-nucleon pairing interaction in the shell, which causes nucleons to form zero total angular momentum pairs. This way, one can, for instance, resolve the so-called even-odd effect [8], which causes the nuclei with an odd number of nucleons to have a lower binding energy than the average binding energy of two neighboring odd-odd nuclei, the first with one more nucleon, the other with one nucleon less. This effect is explained by a pairing interaction between nucleons, which causes nucleons to pair. Other phenomena such as level density, energy gap in the spectra of deformed nuclei, or the total angular momentum of even-even nuclei may be explained this way [8].

A standard many-body method that aims to treat the pairing interactions is the Bardeen-Cooper-Schrieffer method (BCS). This approximate method originated in solid-state physics as a way to describe the superconducting behavior of materials as discussed in [23]. In the solids, an electron and a time-reversed electron form an interacting pair that traverses the crystal lattice. This interaction then causes the superconducting behavior. In a nutshell, the idea behind the BCS method is to describe these particle pairs as a new sort of fermion-like particles.

The transformation to these particle pairs is called the Bogoljubov transformation

Two-state system pairing

j-shell nucleon pairing

$|j, -m_2\rangle\,|j, -m_1\rangle\,|j,\, m_1\rangle\ \ |j,\, m_2\rangle$
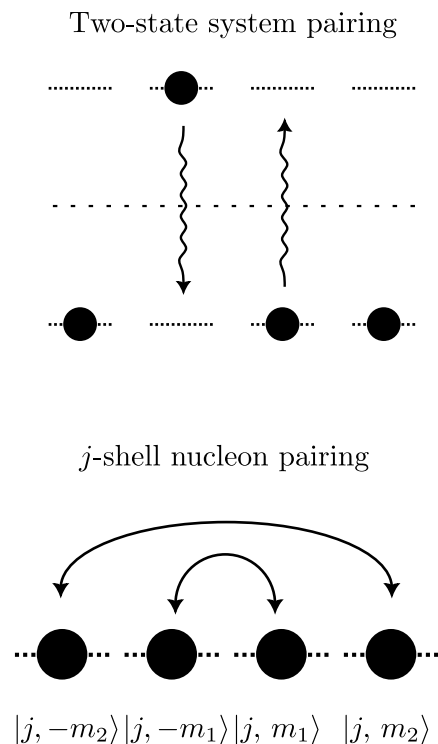
Figure 4.1.1   Two-level system and j-shell pairing.

[8]. For a many-particle system transformed this way, one then seeks to find the ground state energy, or excited states energies by using the variational principles just as in the Hartree-Fock approach. This way, one gets an approximate solution to the original many-body problem. In the following Section 4.2 we introduce the BCS method, following that, in Section 4.3, we apply it to the Lipkin model introduced in Chapter 1.

4.2   General BCS theory

The whole of the BCS method stems from the BCS ground state $|\text{BCS}\rangle$ [8] defined as

$$|\text{BCS}\rangle = \prod_{k>0}^{\Omega/2} \left(u_k + v_k a_k^\dagger a_{\overline{k}}^\dagger \right) |0\rangle, \tag{4.2.1}$$

where u_k^2 and v_k^2 are occupation probabilities for $(k, \overline{k})$ pairs, $|0\rangle$ is the vacuum state and $\Omega/2$ formally denotes the upper boundary of the configuration space which is split in half due to the pairing. The indices k and $\overline{k}$ are conjugated (or simply paired). Usually, we also assume u_k^2 and v_k^2 to be real and positive [8].

We demand the ground state $|\text{BCS}\rangle$ to be normalized

$$\langle \text{BCS}|\text{BCS}\rangle = u_k^2 + v_k^2 = 1 \qquad \forall\,(k, \overline{k}). \tag{4.2.2}$$

Let H be a general two-body interaction Hamiltonian

$$H = \sum_{k_1, k_2 \neq 0}^{\Omega/2} T_{k_1 k_2} a_{k_1}^\dagger a_{k_2} + \frac{1}{4} \sum_{k_1, k_2, k_3, k_4 \neq 0}^{\Omega/2} \overline{V}_{k_1 k_2 k_3 k_4} a_{k_1}^\dagger a_{k_2}^\dagger a_{k_4} a_{k_3}, \tag{4.2.3}$$

with $T_{k_1 k_2}$ and $\overline{V}_{k1 k_2 k_3 k_4}$ being matrix elements of a one-body kinetic energy operator T and a two-body antisymmyetric potential energy operator $\overline{V}$ with $\overline{V}$ being an antisymmetric form of V, that is $\overline{V}_{k_1 k_2 k_3 k_4} = V_{k_1 k_2 k_3 k_4} - V_{k_1 k_2 k_4 k_3}$.

Following [8], it is also convenient to define average particle number N

$$N = \langle \text{BCS}|\widehat{N}|\text{BCS}\rangle = 2 \sum_{k>0}^{\Omega/2} v_k^2, \tag{4.2.4}$$

and particle mean squared error number ΔN as

$$\Delta N = \sqrt{\langle \text{BCS}|\widehat{N}^2 - N^2|\text{BCS}\rangle} = 2 \sqrt{\sum_{k>0}^{\Omega/2} u_k^2 v_k^2}. \tag{4.2.5}$$

The reason for defining the average particle number N is simply because the BCS method does not preserve the correct particle number. To tackle this issue, one needs to solve BCS equations with an additional constraint that fixes the particle number N at its proper mean value.

To set up BCS equations, we define [8] BCS Hamiltonian H_{BCS}

$$H_{\text{BCS}} \equiv H - \lambda N, \tag{4.2.6}$$

with λ being a Lagrange multiplier for the particle number N.

The ground state mean energy [8] is

$$
\begin{aligned}
E_{0,\lambda}^{\text{BCS}} &\equiv \langle \text{BCS}|H_{\text{BCS}}|\text{BCS}\rangle = \\
&= \sum_{k_1 \neq 0}^{\Omega/2} \left[(T_{k_1 k_1} - \lambda)v_{k_1}^2 + \frac{1}{2}\sum_{k_2 \neq 0}^{\Omega/2} \overline{V}_{k_1 k_2 k_1 k_2} v_{k_1}^2 v_{k_2}^2 \right] + \sum_{k_1,k_2>0}^{\Omega/2} \overline{V}_{k_1 \bar{k}_1 k_2 \bar{k}_2} u_{k_1} v_{k_1} u_{k_2} v_{k_2}.
\end{aligned}
$$
(4.2.7)

This particular computation of Eq. (4.2.7) is covered in [22] using a similar notation to ours which originates in [8]. Alternatively, the computation is carried out in [17], which also covers the whole theory of the BCS method and gives several examples of it, however, the used notation is different.

Next we minimize E_0 with respect to Lagrange multiplier λ, which is equivalent to minimizing $E_{0,\lambda}^{\text{BCS}}$ with respect to N

$$
\frac{\mathrm{d}E_0}{\mathrm{d}\lambda}(\lambda) = \lambda \frac{\mathrm{d}N}{\mathrm{d}\lambda} \qquad \Longleftrightarrow \qquad \frac{\mathrm{d}E_{0,\lambda}^{\text{BCS}}}{\mathrm{d}N} = 0.
$$
(4.2.8)

From Eq. (4.2.8) we see the physical meaning of the Lagrange multiplier λ which is just chemical potential, in other words, the energy needed or released upon the addition of a particle to the system.

We also minimize energy $E_{0,\lambda}^{\text{BCS}}$ respect to u_k and v_k

$$
\delta \langle \text{BCS}|H_{\text{BCS}}|\text{BCS}\rangle = \delta E_{0,\lambda}^{\text{BCS}}[u_k, v_k] = 0,
$$
(4.2.9)

which is to be rewritten as

$$
\left(\frac{\partial}{\partial v_k} + \frac{\partial u_k}{\partial v_k}\frac{\partial}{\partial u_k} \right) \langle \text{BCS}|H_{\text{BCS}}|\text{BCS}\rangle = 0.
$$
(4.2.10)

Inserting $E_{0,\lambda}^{\text{BCS}}$ from Eq. (4.2.7) to Eq. (4.2.10) gives the following set of equations

$$
2\widetilde{\varepsilon}_k u_k v_k + \Delta_k(v_k^2 - u_k^2) = 0,
$$
(4.2.11)

$$
\widetilde{\varepsilon}_k = \frac{1}{2}\left[T_{kk} + T_{\bar{k}\bar{k}} + \sum_{k_1>0}^{\Omega/2} \left(V_{kk_1kk_1} + V_{\bar{k}k_1\bar{k}k_1} \right) v_{k_1}^2 \right] - \lambda,
$$
(4.2.12)

$$
\Delta_k = -\sum_{k_1>0}^{\Omega/2} V_{k\bar{k}k_1\bar{k}_1} u_{k_1} v_{k_1},
$$
(4.2.13)

with $\widetilde{\varepsilon}_k$ and Δ_k just being auxiliary parameters. These equations can be further recast to the form

$$
u_k^2 = \frac{1}{2}\left(1 \pm \frac{\widetilde{\varepsilon}_k}{\sqrt{\widetilde{\varepsilon}_k^2 + \Delta_k^2}} \right),
$$
(4.2.14)

$$
v_k^2 = \frac{1}{2}\left(1 \pm \frac{\widetilde{\varepsilon}_k}{\sqrt{\widetilde{\varepsilon}_k^2 + \Delta_k^2}} \right),
$$
(4.2.15)

The set of Eq. (4.2.11) to Eq. (4.2.15) together with particle number Eq. (4.2.4) produce the set of BCS equations as given in [8, 22]. In general, these are non-linear equations, however, one can in principle always attempt to solve them.

So far, the advertised concept of mutually non-interacting quasi-particles from Section 4.1 has not appeared, or at least not explicitly. Nonetheless, the quasi-particles have been present in the entire theory ever since Eq. (4.2.1).

In fact, new fermion-like particle operators can be introduced by the following [8] Bogoljubov transformation

$$c_k^\dagger = u_k a_k^\dagger - v_k a_{\overline{k}}, \quad c_{\overline{k}}^\dagger = u_k a_{\overline{k}}^\dagger - v_k a_k, \tag{4.2.16}$$

$$c_k = u_k a_k - v_k a_{\overline{k}}^\dagger, \quad c_{\overline{k}} = u_k a_{\overline{k}} - v_k a_k^\dagger, \tag{4.2.17}$$

which do satisfy fermion anti-commutation relations

$$\{c_k, c_l^\dagger\} = \delta_{kl}, \quad \{c_k, c_l\} = \{c_k^\dagger, c_l^\dagger\} = 0. \tag{4.2.18}$$

In particular, the BCS ground state $|\text{BCS}\rangle$ [8] turns out to be just a mean-field ground state for these quasi-particles

$$|\text{BCS}\rangle \sim \prod_k^{\Omega/2} c_k^\dagger |0\rangle, \tag{4.2.19}$$

$$c_k |\text{BCS}\rangle = 0, \ \forall k. \tag{4.2.20}$$

Although we do not explicitly make any use of the concept of quasi-particles as such in the present thesis, it may be good to have this concept in mind, as it certainly gives an insight into the background of the BCS method[1].

4.3 BCS method in the Lipkin model

We apply the BCS method presented in Section 4.2 to the specific case Lipkin model introduced in Chapter 1 with the interaction V turned off. We start by taking energy operator H from Eq. (1.1.7) and setting $V = 0$

$$
\begin{aligned}
H = {} & \frac{\varepsilon}{2} \sum_n^\Omega \left(a_{n+}^\dagger a_{n+} - a_{n-}^\dagger a_{n-} \right) - \\
& - \frac{W}{2} \sum_{n,m}^\Omega \left(a_{n+}^\dagger a_{m-}^\dagger a_{m+} a_{n-} + a_{n-}^\dagger a_{m+}^\dagger a_{m-} a_{n+} \right).
\end{aligned} \tag{4.3.1}
$$

We limit ourselves to a model with pure interaction W because it strongly resembles some pairing interaction between the two levels of the system. To some extent, we already saw this in Section 1.2 when discussing the odd-even effect analogy.

For brevity, we label the two pairing indices $(k, \overline{k})$ as $(k+, k-)$, in other words, we want to describe a pairing between the lower and upper shells.

---

[1]When evaluating $E_{0,\lambda}^{\text{BCS}}$ ground state energy from Eq. (4.2.8), using the quasi-particle formalism [22] makes it significantly easier to carry out the calculation.

Just as in Eq. (4.2.1), we assume the $|\text{BCS}\rangle$ ground state to be

$$|\text{BCS}\rangle = \prod_{k=1}^{N}(u_{k+} + v_{k+}a_{k+}^{\dagger}a_{k-}^{\dagger})|0\rangle, \tag{4.3.2}$$

with $u_{k\pm}^2$ and $v_{k\pm}^2$ being the occupation probabilities of the upper and the lower shell

$$u_{k\pm}^2 + v_{k\pm}^2 = 1, \quad \forall k = 1, 2, \ldots, N. \tag{4.3.3}$$

Considering the both levels, from Eq. (4.2.4) we get the particle number N added for both levels

$$2\sum_{k=1}^{N}\left(v_{k+}^2 + v_{k-}^2\right) = 2N. \tag{4.3.4}$$

In addition to that we also assume all the $u_{k\pm}^2$ and $v_{k\pm}^2$ to be k-independent, that is

$$v_{k\pm} = v_{l\pm}, \qquad u_{k\pm} = u_{l\pm}, \quad \forall k, l. \tag{4.3.5}$$

Eq. (4.3.5) together with Eq. (4.3.4) immediately imply the following symmetry between the two levels

$$u_{k+} = v_{k-}, \qquad u_{k-} = v_{k+}, \tag{4.3.6}$$

which is very natural and only reflects an internal symmetry of the model. Eq. (4.3.6) in some sense also justifies at first the odd choice of taking the sum in Eq. (4.3.4).

Consequently, we have to find the ground state energy $E_{0,\lambda}^{\text{BCS}}$ from Eq. (4.2.7). To find $E_{0,\lambda}^{\text{BCS}}$ we have to evaluate the mean energy for $|\text{BCS}\rangle$, which can be done using the quasi-particle formalism.

However, it is much easier to map Hamiltonian H in Eq. (4.3.1) onto the general Hamiltonian H in Eq. (4.2.3). The mean ground state energy $E_{0,\lambda}^{\text{BCS}}$ is then obtained by making a proper substitution in Eq. (4.2.7).

Following the mapping procedure, for $E_{0,\lambda}^{\text{BCS}}$ we get

$$E_{0,\lambda}^{\text{BCS}} = \sum_{k=1}^{N}\left[\left(\frac{\varepsilon}{2} - \lambda\right)v_+^2 + \left(-\frac{\varepsilon}{2} - \lambda\right)v_-^2\right] - \frac{W}{2}\sum_{k=1}^{N}\left[v_+^4 + v_+^2 v_-^2 + v_-^4\right] - \\ - W\sum_{k,l=1}^{N}u_+v_+u_-v_-. \tag{4.3.7}$$

Eq. (4.3.7) is then further simplified to the form of

$$E_{0,\lambda}^{\text{BCS}} = \left[\left(\frac{\varepsilon}{2} - \lambda\right)\left(1 - v_-^2\right) + \left(-\frac{\varepsilon}{2} - \lambda\right)v_-^2\right] - \frac{WN}{2}\left[\left(1 - v_-^2\right)^2 + v_-^2\left(1 - v_-^2\right) + \\ + v_-^4\right] - -WN^2 v_-^2\left(1 - v_-^2\right). \tag{4.3.8}$$

47

In the next step, just as in Section 4.2 we minimize $E_{0,\lambda}^{\mathrm{BCS}}$ with respect to the occupation amplitude v_- and particle number N

$$\frac{\mathrm{d}E_{0,\lambda}^{\mathrm{BCS}}}{\mathrm{d}v_-} = 0, \tag{4.3.9}$$

$$\frac{\mathrm{d}E_{0,\lambda}^{\mathrm{BCS}}}{\mathrm{d}N} = 0. \tag{4.3.10}$$

Doing the calculations involved in Eq. (4.3.9) and Eq. (4.3.10) yields the occupation amplitudes to be

$$v_-^2 = u_+^2 = \frac{1}{2}\left(1 + \frac{2\varepsilon}{W(2N-1)}\right), \tag{4.3.11}$$

$$u_-^2 = v_+^2 = \frac{1}{2}\left(1 - \frac{2\varepsilon}{W(2N-1)}\right). \tag{4.3.12}$$

The other part of the solution is chemical potential λ. Since we do not explicitly need to make any use of λ, we do not discuss its properties in present Section 4.3 (for some details concerning λ see Appendix A).

It is instructive to substitute the result of Eq. (4.3.11) and Eq. (4.3.12) to Eq. (4.3.8). To Eq. (4.3.8) we also add total chemical potential λN, and we get

$$E_0^{\mathrm{BCS}} = E_{0,\lambda}^{\mathrm{BCS}} + \lambda N = -N\left[\frac{4\varepsilon^2 + W^2\left(4N^2 + 4N - 3\right)}{8W(2N-1)}\right]. \tag{4.3.13}$$

For discussion of the BCS solution, we also calculate gap parameter Δ and particle fluctuation number ΔN. From Eq. (4.2.13) we get Δ which is same for both levels

$$\Delta = \frac{WN}{2}v_-\sqrt{1 - v_-^2} = \frac{WN}{4}\sqrt{1 - \frac{4\varepsilon^2}{W^2(2N-1)^2}}, \tag{4.3.14}$$

and from Eq. (4.2.5) particle fluctuation number is

$$\Delta N = \sqrt{4Nv_-^2\left(1 - v_-^2\right)} = \sqrt{N - \frac{4\varepsilon^2}{W^2(2N-1)^2}}. \tag{4.3.15}$$

For both quantities Δ and ΔN, it turns out to be particularly useful to take the following two limits [17]

$$\lim_{W\to+\infty}\frac{\Delta}{W}(W) = \frac{N}{4}, \tag{4.3.16}$$

$$\lim_{W\to+\infty}\frac{\Delta N}{N}(W) = \frac{1}{\sqrt{N}}, \tag{4.3.17}$$

which have a very distinctive meaning. Quantity $\Delta N/N$ can be viewed as a relative particle number error, and as we will see, it very well correlates with the actual error of the BCS approximation with respect to the exact solution. The other quantity Δ/W gives a relative energy of the pairing interaction. Two quantities from Eq. (4.3.16) and Eq. (4.3.17) are both plotted in Fig. 4.3.1 as functions of w for different values of particle number N. Both of these quantities have well-defined limits as $w \to +\infty$, which are visualized as red asymptotes.
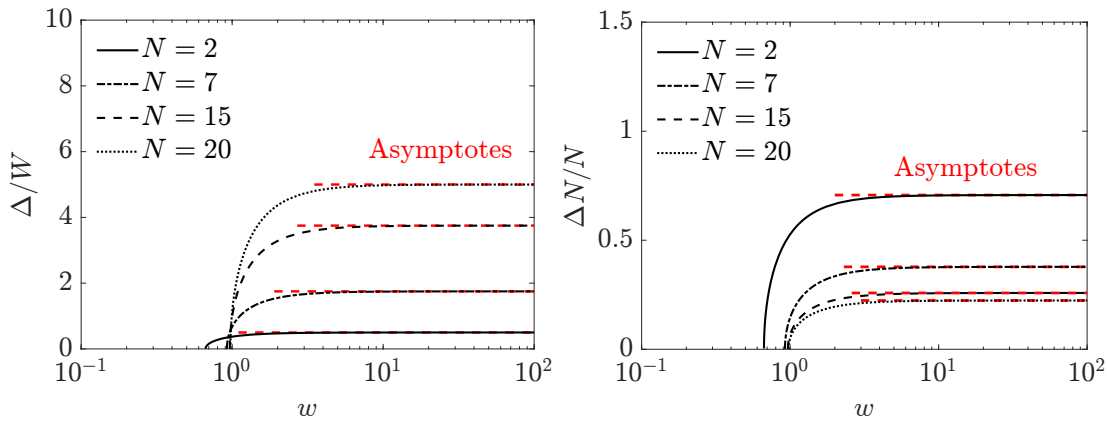
Figure 4.3.1 Left panel shows relative energy gap Δ/W with respect to W for different values of particle number N as a function of interaction strength w. Right panel displays relative particle fluctuation number $\Delta N/N$ for different values of particle number N as a function of interaction strength w.

Lastly, we discuss the existence of BCS solutions and their connection to the HF solution from Chapter 2. From Eq. (4.3.12) we notice v_+^2 and u_-^2 amplitudes to be well defined if and only if

$$W \geq \frac{2\varepsilon}{2N-1}, \tag{4.3.18}$$

which in terms of w is equivalent to

$$w \geq 2\left(\frac{N-1}{2N-1}\right) \equiv w^\star. \tag{4.3.19}$$

Thus from Eq. (4.3.19) we see there exists a BCS solution only if $w \geq w^\star$. If however $w \leq w^\star$, with $w^\star$ being the critical value of interaction strength w, this implies that the occupation amplitudes v_+^2 are trivially zero. This way, it can be shown [8] that ansatz in Eq. (4.3.2) reduces just to the HF mean-field ground state $|\mathrm{HF}\rangle$ in Eq. (2.2.6). The approximate solution to the ground state energy is then given by E_0^{HF} in Eq. (2.3.22). In the left panel in Fig. 4.3.2, we plot the properly extended occupation amplitudes $v_\pm^2$ for both levels as functions of w for three different particle numbers N.

Taking the limit $N \to +\infty$, we see $w^\star \to 1^-$. Taking the same limit, from Eq. (4.3.17) we also get $\Delta N/N \to 0^+$. In conclusion, we see that the BCS transition point (TP) at $w = w^\star$ is equivalent to the PT point which occurs in the exact solution of the Lipkin model. This gives us a hint, that in the limit $N \to +\infty$, the BCS solution tends to reproduce the exact solution including the first PT point at $w = 1$. This, however, is true only for $w \leq 1$, or $w \approx 1$ values, because clearly, the BCS solution does not properly reproduce other PTs taking place in the Lipkin model ground state energy, displayed in Fig. 1.1.1 for particle number $N = 7$. It is also worth noting that for $w \leq 1$ the HF ground state energy E_0^{HF} properly reproduces exact ground state energy E_0.

In the right plot of Fig. 4.3.2 we compare relative energy error $|\Delta E_0|/E_0$ of the ground state energy for all the methods used in the thesis as a function of N for $w = 5$. In Fig. 4.3.3 we compare the BCS solutions to the exact and to
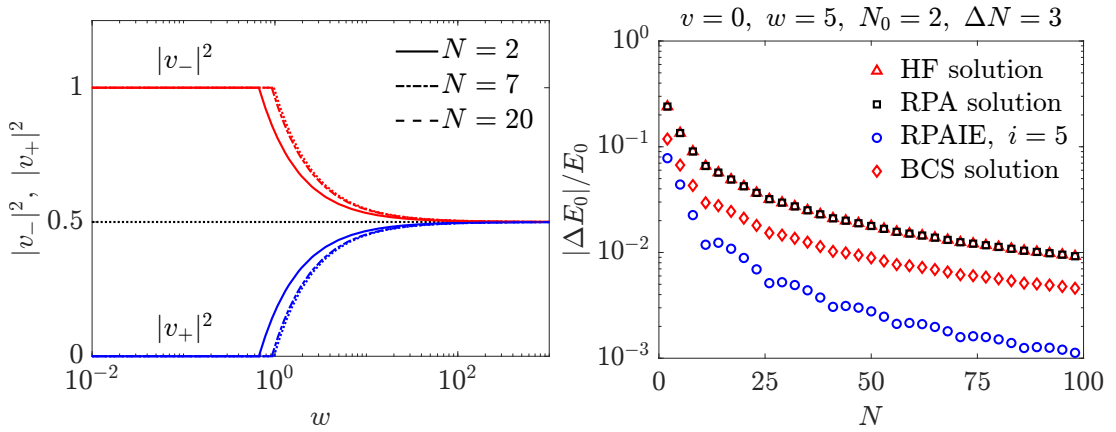
Figure 4.3.2 Left panel displays BCS solution amplitudes $v_\pm^2$ for the upper and the lower level for different values of particle number N as functions of w, with $v_\pm^2$ being either 0 or 1 for $w \leq w^\star$. Right panel shows relative energy error $|\Delta E_0|/E_0$ of the given approximate methods for $w = 5$ as a function of particle number N.

the RPA solution for different values of particle number N as a function of w, in the right panel we compare relative energy error $|\Delta E_0|/E_0$ of the RPA, RPAIE, and BCS methods for different values of particle number N for values $w \geq w^\star$. From all the plots in Fig. 4.3.3 we deduce the BCS approximation to give a better solution to the ground state energy than the standard RPA method, moreover for large values of w we see the RPAIE method to always give a better result. From Fig. 4.3.2 we notice that for large values of N the RPAIE method also produces a better solution than the BCS method. We can also see that both the HF and RPA methods give the same result for large values of w. Thus the RPA method can not properly describe the interaction W^2.

Another particularly interesting phenomenon apparent from the right panel in Fig. 4.3.2, is the jumping pattern seen in the RPAIE and the BCS solutions[3]. Something of similar nature appears in Fig. 4.3.3, namely in the plots showing $|\Delta E_0|/E_0$ relative ground state energy error. In Fig. 4.3.3 a similar jumping effect is caused by PTs. This could be the cause of the jumping effect which can be seen in Fig. 4.3.2.

The BCS solution presented in current Section 4.3 seems to be the same as that in [17] although no explicit formula for energy operator H is given there, thus we can just speculate if the two systems are the same. Our results also appear to be similar to that in [18] which provides only few details on the computation and does not give an explicit formula for the ground state energy similar to Eq. (4.3.13) or that in [17].

---

[2]This is true only for pure interaction W. If however interaction V is included, the approximation gets better overall. This most likely happens due to some sort of a coupling between the two interactions which emerges, once both interactions are turned on.

[3]Unfortunately, neither the RPAIE nor BCS solutions manage to reproduce this intriguing behavior, which leads to the jumping effect.
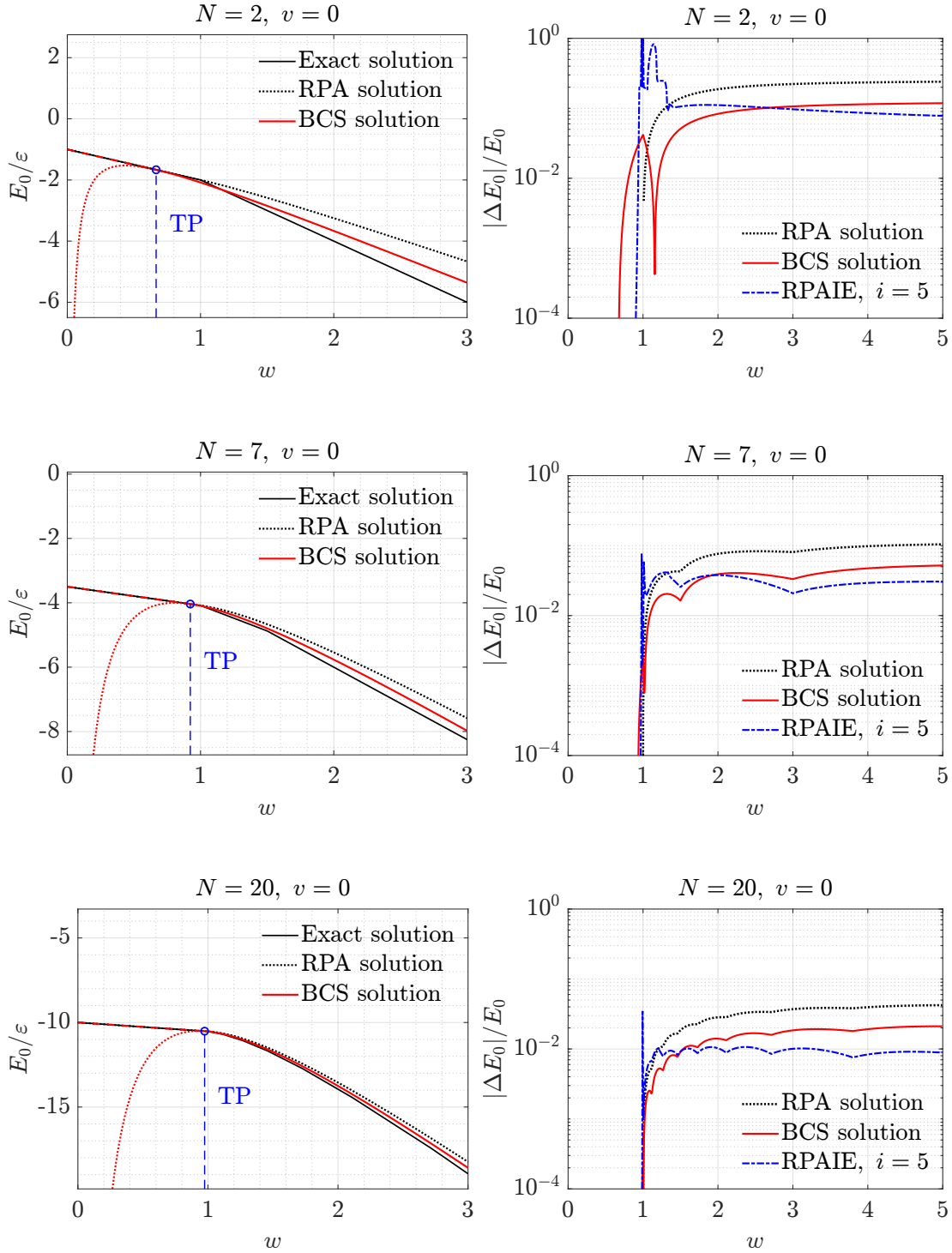
Figure 4.3.3 Left panels show plots of the relative ground state energy E_0/ε for the exact energy (black solid line), the RPA ground state energy (black dotted line), and the BCS ground state energy (red solid line). Right panels display relative ground state energy error for the RPA approximation (black dotted line), the BCS approximation (red solid line), and the RPAIE approximation with $i = 5$ iterations (blue dash-dotted line).

Conclusion

In Chapter 1, we concisely introduced the standard Lipkin model [1]. Section 1.1 was dedicated to a review of the usual quasi-spin algebra solution [1, 10]. Then in Section 1.2 we briefly discussed some of the physical properties of the model. Namely, we pinpointed the existence of phase transitions in the system's ground state energy. An analytic proof for the existence of the first phase transition point for a model with pure interaction W was given. Together with that, we also showed the odd-even effect analogy to appear. We provided an exact explanation of this effect for values of $0 < w < 1$ and $v = 0$. From a numerical solution, we discussed how the effect gets broken or restored as interaction strengths v and w change.

As for Chapter 2, a HF solution within the Lipkin model was established. In short, in Section 2.3 we verified the well-known HF solution [8, 10, 11]. Following that, using the HF solution from Chapter 2 in Chapter 3, we introduced the RPA method. We derived the RPA solution of the Lipkin model, thus validating calculations done in [10, 11]. Having both the RPA and HF solutions in Section 3.3, we compared the two solutions with numerical results of the exact eigenvalue problem.

In the case of the RPA solutions, we further studied their properties. First, we verified QBA and commented on its validity. Then a detailed analysis of the RPA collapse point was made. In particular, for a system without interaction V, we matched the existence of the collapse point to the first phase transition point that occurs in the ground state energy. For a general system, we hypothesize its appearance to be a direct consequence of the HF approximation. As for this hypothesis, the HF solution would have to be reconsidered. More precisely, for values of $v + w \geq 1$, the proper HF ground state may, in fact, be different from that we found in Chapter 2 or in [10, 11]. Although QBA was not valid for all values of v and w, we always found the RPA solution to provide a better approximation to the ground state energy than the HF method. We also included an approximate solution to the first excited state energy obtained by means of the TDA and RPA methods. For low values of v, $w < 1$, we saw these to give a decent estimate of the exact energies, results for both the TDA and RPA methods were similar.

Based on an idea hinted in [8], in Section 3.4, we developed an iterative extension to the usual RPA method which we called the RPAIE method. We gave a procedure to solve for the ground state energy of the Lipkin model using the RPAIE method. We plotted several numerical solutions of the ground state energy using the RPAIE method. Following that, a comprehensive comparison of the ground state energy approximation quality for the RPAIE method with respect to the RPA and HF methods was provided. We conclude the RPAIE method with a sufficient number of iterations $i = 5$ to be superior to the RPA

method for both small and large values of v and w parameters. Moreover, the RPAIE solution converges faster than both the HF and RPA solutions as particle number N increases.

Last Chapter 4 was only concerned with treating interaction W. Realizing the interaction to be a kind of pairing interaction, we tackled the Lipkin model with pure interaction W using the BCS method. In Section 4.3, we derived a corresponding BCS solution. Next, we commented upon some of the properties of the BCS solutions. First, we discussed the existence of the BCS solution and its reduction to the HF solution when $w < w^\star$. We then explored the BCS solution and compared it to that of the RPAIE, RPA, and HF methods. The BCS solution yields a better estimate of the ground state energy than both the RPA and HF methods, however, for large values of w or N, it becomes inferior to the RPAIE method. From the plotted numerical solution, we deduced the BCS solution error to directly correlate with relative particle number error $\Delta N/N$, as expected.

Turning to the future, more attention could go to the mean-field approximation. Possibly more sophisticated mean-field methods such as the Hartree-Fock-Bogoljubov method [8] that combines both the BCS and HF methods [17] may be employed. On top of that, the classical HF solution could be re-evaluated. Aside from that, the proposed RPAIE method appears to be a promising improvement to the standard RPA method. In particular, it may be worth testing the RPAIE method with other possibly more complicated models. In the case of the BCS method, the quasi-particle formalism from Section 4.2 might be used to solve for the energies of the excited states. One could also opt for similar BCS-like methods or extensions such as the Lipkin-Nogami BCS method [17]. Going the other way around, the original two-level model [1] may be extended in many ways. For example, new types of interactions, such as those in [11], may be included. Notably, adding a three-body interaction to the Lipkin model could be an intriguing subject of future research. Alternatively, more levels may be added to the system [13–15].

Bibliography

1. Lipkin, H. J., Meshkov, N. & Glick, A. J. Validity of many-body approximation methods for a solvable model, (I). Exact solution and perturbation theory. *Nuclear Physics* **62,** 188–198 (1965).

2. Lipkin, H. J., Meshkov, N. & Glick, A. J. Validity of many-body approximation methods for a solvable model, (II). Linearization procedures. *Nuclear Physics* **2,** 199–210 (1965).

3. Lipkin, H. J., Meshkov, N. & Glick, A. J. Validity of many-body approximation methods for a solvable model, (III). Diagram summations. *Nuclear Physics* **62,** 211–224 (1964).

4. Mielke, A. Flow equations for band-matrices. *The European Physical Journal B - Condensed Matter and Complex Systems* **5,** 605–611 (1998).

5. Morrison, S. & Parkins, A. S. Dynamical Quantum Phase Transitions in the Dissipative Lipkin-Meshkov-Glick Model with Proposed Realization in Optical Cavity QED. *Physical Review Letters* **100,** 040403 (2008).

6. Cervia, M. J. *et al.* Lipkin model on a quantum computer. *Physical Review C* **104,** 024305 (2021).

7. Heiss, W. D., Scholtz, F. G. & Geyer, H. B. The large N behaviour of the Lipkin model and exceptional points. *Journal of Physics A: Mathematical and General Physics* **38,** 1843–1851 (2005).

8. Ring, P. & P.Shuck. *The Nuclear Many-Body Problem* (Springer-Verlag New York Inc., 1980).

9. Plastino, A. & Moszkowski, S. A. Simplified Model for mustrating Hartree-Fock in a Lipkin-Model Problem. *Il Nuovu Cimento A* **47,** 470–474 (1978).

10. Co', G. & Leo, S. D. Hartree-Fock and Random Phase Approximation theories in a many-fermion solvable model. *Modern Physics Letter A* **30,** 1550196 (2015).

11. Romano, R. *Master thesis - A generalization of the Lipkin model as a testing ground for many-body theories* `https://www0.mi.infn.it/~jroca/doc/thesis/thesis-riccardo-romano-magistrale.pdf`.

12. Papakonstantinou, P. Second random-phase approximation, Thouless' theorem, and the stability condition reexamined and clarified. *Physical Review C* **90,** 024305 (2014).

13. Grasso, M., Catara, F. & Sambataro, M. Boson-mapping-based extension of the random-phase approximation in a three-level Lipkin model. *Physical Review C* **66,** 064303 (2002).

14. Hagino, K. & Bertsch, G. F. Random-phase approximation approach to rotational symmetry restoration in a three-level Lipkin model. *Physical Review C* **61,** 024307 (2000).

15. Delion, D. S., Schuck, P. & Dukelsky, J. Self-consistent random phase approximation and the restoration of symmetries within the three-level Lipkin model. *Physical Review C* **72,** 064305 (2005).

16. Terasaki, J. *et al.* Reproduction of exact solutions of Lipkin model by nonlinear higher random-phase approximation. *International Journal of Modern Physics E,* 1750062 (2017).

17. Suhonen, J. *From Nucleaons to Nucleus: Concepts of Microscopic Nuclear Theory* (Springer, 2007).

18. Betan, R. M. I. Comparison between the Lipkin-Nogami and Richardson solutions with complex single particle energy in the Lipkin's model. *arXiv:1710.07570 [nucl-th].* https://arxiv.org/abs/1710.07570 (2017).

19. Debergh, N. & Stancu, F. On the exact solutions of the Lipkin-Meshkov-Glick model. *Journal of Physics A: Mathematical and General Physics* **34,** 3265–3276 (2018).

20. Sakurai, J. *Modern Quantum Mechanics* (Addison - Wesley Publishing Company, 1994).

21. Cejnar, P. *A Condensed Course of Quantum Mechanics* (Karolinum, 2013).

22. Rowe, D. J. *Nuclear Collective Motion* (World Scientific Publishing Co. Pte. Ltd., 2010).

23. Feynman, R. P. *Statistical Mechanics: A Set of Lectures* (The Benjamin/Cummings Publishing Company, Inc., 1972).

Appendix A

Auxiliary formulae and calculations

Appendix A contains all the auxiliary formulae and calculations gathered from all the chapters of the present thesis. These were mostly straightforward to carry out, but we found it inappropriate to plague the main text with those due to their length.

Chapter 1 - Exact solutions

Evaluation of anti-commutator in Section 1.2 is

$$(K_+ K_- + K_- K_+)\, |k,\, m\rangle = \left[\sqrt{(k+m)(k-m+1)(k-m+1)(k+m)}+\right.$$

$$\left.+\sqrt{(k-m)(k+m+1)(k+m+1)(k-m)}\right] =$$

$$= [(k+m)(k-m+1) + (k-m)(k+m+1)]\, |k,\, m\rangle =$$

$$= 2\left[k(k+1) - m^2\right] |k,\, m\rangle.$$

Chapter 2 - HF method

First, we give an explicit computation for the transformation of K_0 and $K_\pm$ operators. We start with K_0

$$K_0 = \frac{1}{2}\sum_n^\Omega \left(a_{n+}^\dagger a_{n+} - a_{n-}^\dagger a_{n-}\right) = \frac{1}{2}\sum_n^\Omega \left\{\left[\cos^2(\beta) - \sin^2(\beta)\right] \cdot\right.$$

$$\cdot \left(\widetilde{a}_{n+}^\dagger \widetilde{a}_{n+} - \widetilde{a}_{n-}^\dagger \widetilde{a}_{n-}\right) + 2\sin(\beta)\cos(\beta)\left[\widetilde{a}_{n+}^\dagger \widetilde{a}_{n-} + \widetilde{a}_{n-}^\dagger \widetilde{a}_{n+}\right]\right\} =$$

$$= \cos(2\beta)\widetilde{K}_0 + \frac{1}{2}\sin(2\beta)\left[\widetilde{K}_+ + \widetilde{K}_-\right],$$

K_+ follows as

$$K_+ = \sum_n^\Omega a_{n+}^\dagger a_{n-} = \sum_n^\Omega \left[\cos(\beta)\widetilde{a}_{n+}^\dagger + \sin(\beta)\widetilde{a}_{n-}^\dagger\right]\left[-\sin(\beta)\widetilde{a}_{n+} + \cos(\beta)\widetilde{a}_{n-}\right] =$$

$$= \sum_n^\Omega \left\{\cos^2(\beta)\widetilde{a}_{n+}^\dagger\widetilde{a}_{n-} - \sin^2(\beta)\widetilde{a}_{n-}^\dagger\widetilde{a}_{n+} + \sin(\beta)\cos(\beta)\cdot\right.$$

$$\left.\cdot\left[\widetilde{a}_{n-}^\dagger\widetilde{a}_{n-} - \widetilde{a}_{n+}^\dagger\widetilde{a}_{n+}\right]\right\} = \cos^2(\beta)\widetilde{K}_+ - \sin^2(\beta)\widetilde{K}_- + \sin(2\beta)\widetilde{K}_0,$$

fortunately, K_- is easy to get thanks to $(K_+)^\dagger = K_-$ property

$$K_- = \cos^2(\beta)\widetilde{K}_- - \sin^2(\beta)\widetilde{K}_+ + \sin(2\beta)\widetilde{K}_0.$$

When searching for $\widetilde{H}$ expressed in the HF mean-field basis, we need $K_\pm K_\mp$ and $K_\pm^2$ operators and their sums. K_+K_- is

$$K_+K_- = \frac{1}{4}\left[(\cos(\alpha) - 1)\,\widetilde{K}_+^2 + \left(\cos^2(\alpha) - 1\right)\widetilde{K}_-^2 + 4\sin^2(\alpha)\widetilde{K}_0^2 +\right.$$

$$+ (\cos(\alpha) + 1)^2\,\widetilde{K}_+\widetilde{K}_- + (\cos(\alpha) - 1)^2\,\widetilde{K}_-\widetilde{K}_+ + 2\sin(\alpha)(\cos(\alpha) + 1)\,\widetilde{K}_+\widetilde{K}_0 +$$

$$+ 2\sin(\alpha)(\cos(\alpha) - 1)\,\widetilde{K}_0\widetilde{K}_+ + 2\sin(\alpha)(\cos(\alpha) - 1)\,\widetilde{K}_-\widetilde{K}_0 +$$

$$\left.+ 2\sin(\alpha)(\cos(\alpha) + 1)\,\widetilde{K}_0\widetilde{K}_-\right].$$

One obtains K_-K_+ just as easily

$$K_-K_+ = \frac{1}{4}\left[(\cos(\alpha) - 1)\,\widetilde{K}_+^2 + \left(\cos^2(\alpha) - 1\right)\widetilde{K}_-^2 + 4\sin^2(\alpha)\widetilde{K}_0^2 +\right.$$

$$+ (\cos(\alpha) - 1)^2\,\widetilde{K}_+\widetilde{K}_- + (\cos(\alpha) + 1)^2\,\widetilde{K}_-\widetilde{K}_+ + 2\sin(\alpha)(\cos(\alpha) - 1)\,\widetilde{K}_+\widetilde{K}_0 +$$

$$+ 2\sin(\alpha)(\cos(\alpha) + 1)\,\widetilde{K}_0\widetilde{K}_+ + 2\sin(\alpha)(\cos(\alpha) + 1)\,\widetilde{K}_-\widetilde{K}_0 +$$

$$\left.+ 2\sin(\alpha)(\cos(\alpha) - 1)\,\widetilde{K}_0\widetilde{K}_-\right].$$

We now compute the sum $K_+K_- + K_-K_+$

$$K_+K_- + K_-K_+ = \frac{1}{2}\left(\cos^2(\alpha) - 1\right)\left(\widetilde{K}_+^2 + \widetilde{K}_-^2\right) + 2\sin^2(\alpha)\widetilde{K}_0^2 +$$

$$+ \frac{1}{2}\left(\cos^2(\alpha) + 1\right)\left\{\widetilde{K}_+, \widetilde{K}_-\right\} + \sin(\alpha)\cos(\alpha)\left[\left\{\widetilde{K}_+, \widetilde{K}_0\right\} + \left\{\widetilde{K}_-, \widetilde{K}_0\right\}\right].$$

Next, we need the quadratic terms $K_\pm^2$. The K_+^2 term reads

$$K_+^2 = \frac{1}{4}\left[(\cos(\alpha) + 1)\,\widetilde{K}_+ + 2\sin(\alpha)\widetilde{K}_0 + (\cos(\alpha) - 1)\,\widetilde{K}_-\right]^2 =$$

$$= \frac{1}{4}\left[(\cos(\alpha) + 1)^2\,\widetilde{K}_+^2 + (\cos(\alpha) - 1)^2\,\widetilde{K}_-^2 + 4\sin^2(\alpha)\widetilde{K}_0^2 +\right.$$

$$+ \left(\cos^2(\alpha) - 1\right)\left\{\widetilde{K}_+, \widetilde{K}_-\right\} + 2\sin(\alpha)(\cos(\alpha) + 1)\left\{\widetilde{K}_+, \widetilde{K}_0\right\} +$$

$$\left.+ 2\sin(\alpha)(\cos(\alpha) - 1)\left\{\widetilde{K}_-, \widetilde{K}_0\right\}\right],$$

and K_-^2 follows as

$$K_-^2 = \frac{1}{4}\left[(\cos(\alpha) + 1)\,\widetilde{K}_- + 2\sin(\alpha)\widetilde{K}_0 + (\cos(\alpha) - 1)\,\widetilde{K}_+\right]^2 =$$

$$= \frac{1}{4}\left[(\cos(\alpha) + 1)^2\,\widetilde{K}_-^2 + (\cos(\alpha) - 1)^2\,\widetilde{K}_+^2 + 4\sin^2(\alpha)\widetilde{K}_0^2 + \right.$$

$$+ \left(\cos^2(\alpha) - 1\right)\left\{\widetilde{K}_+,\,\widetilde{K}_-\right\} + 2\sin(\alpha)\left(\cos(\alpha) + 1\right)\left\{\widetilde{K}_-,\,\widetilde{K}_0\right\} +$$

$$\left. + 2\sin(\alpha)\left(\cos(\alpha) - 1\right)\left\{\widetilde{K}_+,\,\widetilde{K}_0\right\}\right].$$

The sum is

$$K_+^2 + K_-^2 = \frac{1}{2}\left(\cos^2(\alpha) + 1\right)\left(\widetilde{K}_+^2 + \widetilde{K}_-^2\right) + 2\sin^2(\alpha)\widetilde{K}_0^2 +$$

$$+ \frac{1}{2}\left(\cos^2(\alpha) - 1\right)\left\{\widetilde{K}_+,\,\widetilde{K}_-\right\} + 4\sin(\alpha)\cos(\alpha)\left[\left\{\widetilde{K}_-,\,\widetilde{K}_0\right\} + \left\{\widetilde{K}_+,\,\widetilde{K}_0\right\}\right].$$

Having all the operators above, we write $\widetilde{H}$

$$\widetilde{H} = \frac{\varepsilon}{2}\left[\sin(\alpha)\widetilde{K}_+ + 2\cos(\alpha)\widetilde{K}_0 + \sin(\alpha)\widetilde{K}_-\right] -$$

$$- \frac{W}{2}\left\{\frac{1}{2}\left(\cos(\alpha) - 1\right)\left(\widetilde{K}_+^2 + \widetilde{K}_-^2\right) + 2\sin^2(\alpha)\widetilde{K}_0^2 + \right.$$

$$\left. + \frac{1}{2}\left(\cos(\alpha) + 1\right)\left\{\widetilde{K}_+,\,\widetilde{K}_-\right\} + \sin(\alpha)\cos(\alpha)\left[\left\{\widetilde{K}_+,\,\widetilde{K}_0\right\} + \left\{\widetilde{K}_-,\,\widetilde{K}_0\right\}\right]\right\} -$$

$$- \frac{V}{8}\left\{2\left(\cos^2(\alpha) + 1\right)\left(\widetilde{K}_+^2 + \widetilde{K}_-^2\right) + 8\sin^2(\alpha)\widetilde{K}_0^2 + \right.$$

$$\left. + 2\left(\cos^2(\alpha) - 1\right)\left\{\widetilde{K}_+,\,\widetilde{K}_-\right\} + 4\sin(\alpha)\cos(\alpha)\left[\left\{\widetilde{K}_+,\,\widetilde{K}_0\right\} + \left\{\widetilde{K}_-,\,\widetilde{K}_0\right\}\right]\right\}.$$

Which can be further simplified into a more convenient form of

$$\widetilde{H} = \frac{\varepsilon}{2}\left[\sin(\alpha)\left(\widetilde{K}_+ + \widetilde{K}_-\right) + 2\cos(\alpha)\widetilde{K}_0\right] - \frac{W + V}{4}\left[\left(1 + \cos^2(\alpha)\right)\left(\widetilde{K}_+^2 + \widetilde{K}_-^2\right)\right.$$

$$\left. - \sin(2\alpha)\left(\left\{\widetilde{K}_+,\,\widetilde{K}_0\right\} + \left\{\widetilde{K}_-,\,\widetilde{K}_0\right\}\right) + \sin^2(\alpha)\left(4\widetilde{K}_0^2 - \left\{\widetilde{K}_+,\,\widetilde{K}_-\right\}\right)\right] +$$

$$+ \frac{W}{2}\left[\widetilde{K}_+^2 + \widetilde{K}_-^2 - \left\{\widetilde{K}_+,\,\widetilde{K}_-\right\}\right].$$

Chapter 3 - RPA method

For clarity, the HF mean-field ground state was $|\text{HF}\rangle = |\widetilde{k} = N/2, \widetilde{m} = -N/2\rangle$. To evaluate the RPA equations containing the transformed Hamiltonian $\widetilde{H}$ we

need the following commutators:

$$\left[\widetilde{K}_-, \left[\widetilde{K}_0, \widetilde{K}_+\right]\right] = \left[\widetilde{K}_-, \widetilde{K}_+\right] = -2\widetilde{K}_0,$$

$$\left[\widetilde{K}_-, \left[\widetilde{K}_0^2, \widetilde{K}_+\right]\right] = \left[\widetilde{K}_-, \widetilde{K}_0\left[\widetilde{K}_0, \widetilde{K}_+\right] + \left[\widetilde{K}_0, \widetilde{K}_+\right]\widetilde{K}_0\right] =$$
$$= \left[\widetilde{K}_-, \widetilde{K}_0\widetilde{K}_+ + \widetilde{K}_+\widetilde{K}_0\right] =$$
$$= \left(\widetilde{K}_0\left[\widetilde{K}_-, \widetilde{K}_+\right] + \left[\widetilde{K}_-, \widetilde{K}_0\right]\widetilde{K}_+ + \widetilde{K}_+\left[\widetilde{K}_-, \widetilde{K}_0\right] + \left[\widetilde{K}_-, \widetilde{K}_+\right]\widetilde{K}_0\right) =$$
$$= -4\widetilde{K}_0^2 + \widetilde{K}_-\widetilde{K}_+ + \widetilde{K}_+\widetilde{K}_- = -4\widetilde{K}_0^2 + \{\widetilde{K}_+, \widetilde{K}_-\},$$

$$\left[\widetilde{K}_-, \left[\{\widetilde{K}_+, \widetilde{K}_-\}, \widetilde{K}_+\right]\right] = \left[\widetilde{K}_-, \left[\widetilde{K}_+\widetilde{K}_- + \widetilde{K}_-\widetilde{K}_+, \widetilde{K}_+\right]\right] =$$
$$= \left[\widetilde{K}_-, \widetilde{K}_+\left[\widetilde{K}_-, \widetilde{K}_+\right] + \left[\widetilde{K}_-, \widetilde{K}_+\right]\widetilde{K}_+\right] =$$
$$= -2\left(\widetilde{K}_+\left[\widetilde{K}_-, \widetilde{K}_0\right] + \left[\widetilde{K}_-, \widetilde{K}_+\right]\widetilde{K}_0 + \widetilde{K}_0\left[\widetilde{K}_-, \widetilde{K}_+\right] + \left[\widetilde{K}_-, \widetilde{K}_0\right]\widetilde{K}_+\right) =$$
$$= 8\widetilde{K}_0^2 - 2\{\widetilde{K}_+, \widetilde{K}_-\},$$

$$\left[\widetilde{K}_-, \left[\widetilde{K}_+^2, \widetilde{K}_+\right]\right] = \left[\widetilde{K}_-, \widetilde{K}_+\left[\widetilde{K}_+, \widetilde{K}_-\right] + \left[\widetilde{K}_+, \widetilde{K}_-\right]\widetilde{K}_+\right] =$$
$$= 2\left[\widetilde{K}_-, \widetilde{K}_+\widetilde{K}_0 + \widetilde{K}_0\widetilde{K}_+\right] = -8\widetilde{K}_0^2 + 2\{\widetilde{K}_+, \widetilde{K}_-\},$$

with their aid, it is straightforward to evaluate the following matrix elements

$$\langle HF| \left[\widetilde{K}_-, \left[\widetilde{K}_0, \widetilde{K}_+\right]\right] |HF\rangle = N,$$
$$\langle HF| \left[\widetilde{K}_-, \left[\widetilde{K}_0^2, \widetilde{K}_+\right]\right] |HF\rangle = -N(N-1),$$
$$\langle HF| \left[\widetilde{K}_-, \left[\{\widetilde{K}_+, \widetilde{K}_-\}, \widetilde{K}_+\right]\right] |HF\rangle = 2N(N-1),$$
$$\langle HF| \left[\widetilde{K}_-, \left[\widetilde{K}_+^2, \widetilde{K}_+\right]\right] |HF\rangle = -2N(N-1).$$

Having the matrix elements above, we can easily evaluate RPA equations.

The coefficients A and B from the RPA equations can be obtained from

Hamiltonian $\widetilde{H}$ simply as

$$A = \frac{1}{N}\langle\mathrm{HF}|\left[\widetilde{K}_-,\left[\widetilde{H},\widetilde{K}_+\right]\right]|\mathrm{HF}\rangle = \frac{1}{N}\left[\varepsilon N\cos(\alpha) - N(N-1)W+\right.$$
$$\left. +N(N-1)\frac{(V+W)}{2}\sin^2(\alpha) + N(N-1)(V+W)\sin^2(\alpha)\right] =$$
$$= \varepsilon\cos(\alpha) - W(N-1) + \frac{3}{4}(N-1)(V+W)\sin^2(\alpha),$$

$$B = -\frac{1}{N}\langle\mathrm{HF}|\left[\widetilde{K}_-,\left[\widetilde{H},\widetilde{K}_-\right]\right]|\mathrm{HF}\rangle =$$
$$= -\frac{1}{N}\left[-N(N-1)W - N(N-1)\frac{(V+W)}{2}\cos(2\alpha)\right] =$$
$$= (N-1)W - (N-1)\frac{(W+V)}{2}\left[2\cos^2(\alpha) - 1\right],$$

which allows one to substitute both α_I and α_II back to A and B.

Chapter 4 - BCS method

Chemical potential λ was obtained as a byproduct of the BCS solution to the Lipkin model which follows from Eq. (4.3.9) and Eq. (4.3.10). An explicit form of λ reads

$$\lambda = \frac{4\varepsilon^2 - W^2(16N^3 - 4N^2 - 8N + 3)}{8W(2N-1)^2}.$$

The following figure displays λ as a function of either w or N. Chemical potential λ has a distinctive physical meaning as a quantity that tells how much energy is either required or obtained once a particle is added to the system. If one was to consider an open quantum system that is allowed to exchange particles, λ quantity would provide valuable knowledge.
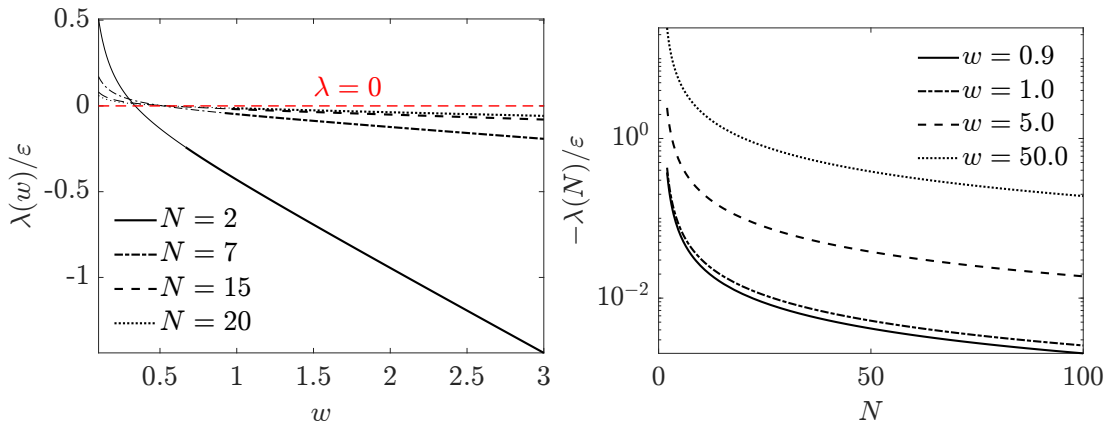
Left panel shows $\lambda(w)/\varepsilon$ plot as a function of w interactions strength. for given values of N. Right panel displays the plot of $\lambda(N)/\varepsilon$ as a function of N particle number for given values of w interaction strength.